








# AUTHOR/EDITOR QUERIES

ARTICLE ID: SYS-syw068			
Please respond to all queries and send any additional proof corrections. Failure to do so could result in delayed publication			
Query No	Section	Paragraph	Query
Q1	Author names		Please check that all names have been spelled correctly and appear in the correct order. Please also check that all initials are present. Please check that the author surnames (family name) have been correctly identified by a pink background. If this is incorrect, please identify the full surname of the relevant authors. Occasionally, the distinction between surnames and forenames can be ambiguous, and this is to ensure that the authors' full surnames and forenames are tagged correctly, for accurate indexing online. Please also check all author affiliations.
Q2			Please provide the definition of GTR, HPD.
Q3			If applicable figures have been placed as close as possible to their first citation. Please check that they are complete and that the correct figure legend is present. Figures in the proof are low resolution versions that will be replaced with high resolution versions when the journal is printed.
Q4			Please check that the text is complete and that all figures, tables and their legends are included.
Q5			This figure is currently intended to appear in color online and black and white in print. Please check the black and white versions at the end of the proof, and if necessary, re-word the text and legend to avoid references to color.
Q6			If you have submitted files to Dryad, please can you check the Dryad URL to make sure it contains the correct doi and is linked to your data package? Please confirm in the proof if it is correct or if it needs to be changed.
Q7			Please check and revise the last page.

# MAKING CORRECTIONS TO YOUR PROOF

**NOT FOR  
PUBLIC RELEASE**

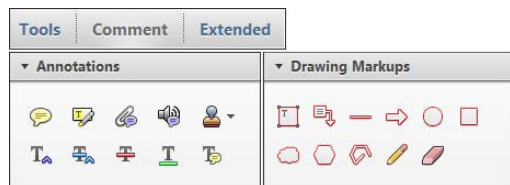
These instructions show you how to mark changes or add notes to the document using the Adobe Acrobat Professional version 7 (or onwards) or Adobe Reader X (or onwards). To check what version you are using go to **Help** then **About**. The latest version of Adobe Reader is available for free from [get.adobe.com/reader](http://get.adobe.com/reader).

## Displaying the toolbars

### Adobe Professional X, XI and Reader X, XI

Select **Comment, Annotations and Drawing Markups**.

If this option is not available, please let me know so that I can enable it for you.



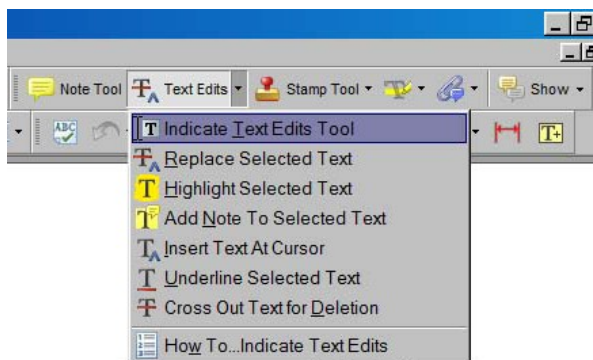
### Acrobat Professional 7, 8 and 9

Select **Tools, Commenting, Show Commenting Toolbar**.



## Using Text Edits

This is the quickest, simplest and easiest method both to make corrections, and for your corrections to be transferred and checked.



1. Click **Text Edits**
2. Select the text to be annotated or place your cursor at the insertion point.
3. Click the **Text Edits** drop down arrow and select the required action.

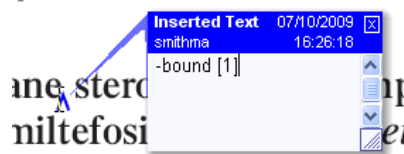
*You can also right click on selected text for a range of commenting options.*

## SAVING COMMENTS

In order to save your comments and notes, you need to save the file (**File, Save**) when you close the document. A full list of the comments and edits you have made can be viewed by clicking on the Comments tab in the bottom-left-hand corner of the PDF.

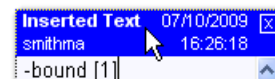
## Pop up Notes

With *Text Edits* and other markup, it is possible to add notes. In some cases (e.g. inserting or replacing text), a pop-up note is displayed automatically.



To **display** the pop-up note for other markup, right click on the annotation on the document and selecting **Open Pop-Up Note**.

To **move** a note, click and drag on the title area.



To **resize** of the note, click and drag on the bottom right corner.



To **close** the note, click on the cross in the top right hand corner.

To **delete** an edit, right click on it and select **Delete**. The edit and associated note will be removed.

Syst. Biol. 0(0):1–25, 2016  
 © The Author(s) 2016. Published by Oxford University Press, on behalf of the Society of Systematic Biologists. All rights reserved.  
 For Permissions, please email: journals.permissions@oup.com  
 DOI:10.1093/sysbio/syw068

## Approaches for Phylogenetic Inference from Morphological Data and Total-Evidence Dating in Squamate Reptiles (Lizards, Snakes, and Amphisbaenians)

R. ALEXANDER PYRON\*

Department of Biological Sciences, The George Washington University, 2023 G St. NW, Washington, DC 20052;

\*Correspondence to be sent to: Department of Biological Sciences, The George Washington University, 2023 G St. NW, Washington, DC 20052;  
 E-mail: rpyron@columboid.org

Received 6 October 2015; reviews returned 12 July 2016; accepted 20 July 2016  
 Associate Editor: Thomas Near

**Abstract.**—Here, I combine previously underutilized models and priors to perform more biologically realistic phylogenetic inference from morphological data, with an example from squamate reptiles. When coding morphological characters, it is often possible to denote ordered states with explicit reference to observed or hypothetical ancestral conditions. Using this logic, we can integrate across character-state labels and estimate meaningful rates of forward and backward transitions from plesiomorphy to apomorphy. I refer to this approach as MkA, for “asymmetric.” The MkA model incorporates the biological reality of limited reversal for many phylogenetically informative characters, and significantly increases likelihoods in the empirical data sets. Despite this, the phylogeny of Squamata remains contentious. Total-evidence analyses using combined morphological and molecular data and the MkA approach tend toward recent consensus estimates supporting a nested Iguania. However, support for this topology is not unambiguous across data sets or analyses, and no mechanism has been proposed to explain the widespread incongruence between partitions, or the hidden support for various topologies in those partitions. Furthermore, different morphological data sets produced by different authors contain both different characters and different states for the same or similar characters, resulting in drastically different placements for many important fossil lineages. Effort is needed to standardize ontology for morphology, resolve incongruence, and estimate a robust phylogeny. The MkA approach provides a preliminary avenue for investigating morphological evolution while accounting for temporal evidence and asymmetry in character-state changes. [Congruence; convergence; dating; molecular discordance; morphological phylogenetics; reversals; Squamata; total evidence.]

A major recent trend in systematics is the reintegration of morphological data into total-evidence phylogenetics (Kluge 1989; Eernisse and Kluge 1993), reuniting paleontology and neontology to build a fully sampled Tree of Life (Giribet 2015; Pyron 2015). These trees offer unparalleled insight into evolutionary history, drastically increasing the power of historical inference (Slater and Harmon 2013) and elucidating evolutionary processes (Wood et al. 2013). Integrating fossil data into phylogenetic inference has long been considered desirable (Gauthier et al. 1988; Huelsenbeck 1991; Eernisse and Kluge 1993; Wagner 1995), though effort waned substantially during the ascendancy of molecular systematics.

A revival has been facilitated by computational methods and mathematical models that account for substitution processes in both discrete morphological characters (Lewis 2001; Wright and Hillis 2014) and DNA-sequence data (Hillis et al. 1996; Felsenstein 2004) in single analyses (Pyron 2011; Ronquist et al. 2012). These methodological developments also highlight several epistemological and philosophical issues regarding incongruence between data types, partitions, and substitution dynamics that have been somewhat overlooked in recent studies (see discussions in Lee and Palci 2015 and O'Reilly et al. 2015).

First, total-evidence dating assumes a morphological clock; that at least to some extent, an observable, calculable substitution process is operating in all data partitions. Total-evidence dating does not actually require molecular data, and could be based on a morphological matrix alone, from which a

morphological clock alone can be estimated (Wagner 1998; Lee et al. 2014; Slater 2015). The morphological clock is a concept that requires further study. Regardless, total-evidence studies generally assume that (i) we observe a set of changes in our morphological character matrix, (ii) these changes have occurred over a set period of time, and (iii) these changes have been more or less orderly, such that a broadly informative rate of morphological change can be estimated to parameterize an overall clock rate.

Second, combining data sources (e.g., morphology and molecules) should help overcome homoplasy. Convergent evolution misleading phylogenetic inference is known to affect both morphological (Wiens et al. 2003, 2005; Wilcox et al. 2004) and molecular (Castoe et al. 2009; Parker et al. 2013; Foote et al. 2015) data sets. Molecular systematists often implicitly assume that DNA-sequence data contain the “true” phylogenetic signal, and this may be the case majority of the time. Regardless, there are still, frequently, deep nodes in the Tree of Life that are not strongly resolved even by genome-scale data (see Pyron 2015). These may be resolved, however, by the addition of quasi-independent signal from morphological data. There still remains a strong possibility of homoplasy in some character suites, such as those related to troglodytism, neoteny, and fossoriality, which may yield incongruent placement for taxa with many convergent character-states (Wiens et al. 2003, 2005, 2010; Wilcox et al. 2004).

Third, total-evidence dating must include stratigraphic data. An explicit, but underappreciated facet of divergence-time estimation, whether using

node-age calibration priors or fossil-tip dating, is that the introduction of an explicit timescale is itself phylogenetically informative, and can alter estimates of both topology and branch lengths (Drummond et al. 2006). For a molecular matrix consisting of only extant taxa, node-age calibrations place a narrower prior on the rate of molecular substitutions, and limit subtending bifurcations to specific time windows. Accordingly, different topologies may have similar likelihoods if not calibrated to time, but may have drastically different likelihoods when ultrametricized, if one conformation implies unlikely rates of change along branches.

This notion has a long precedent in the paleobiological literature (Wagner 1995; Clyde and Fisher 1997; see Smith 1998), resulting in the development of “stratocladistics” to infer fossil relationships while incorporating stratigraphic data (Fisher 2008). A given stratigraphic series can be accommodated by almost any topology if the divergences are stretched back far enough. However, the order of appearance in the fossil record places a strong prior or limit on the expected or likely series of divergence among species, and several methods were developed to account for this (Huelsenbeck 1994; Huelsenbeck and Rannala 1997; Wagner 1998). Ignoring this information has long been known to be potentially misleading (Wagner 2000). Thus, uncalibrated analyses that reveal unorthodox placements of fossil taxa (Wiens et al. 2010; Reeder et al. 2015) may have been misled by inadequate consideration of evolutionary dynamics and incomplete integration of total (e.g., temporal) evidence.

This is also relevant when we consider the priors placed on topologies and divergence times in a Bayesian total-evidence framework. A total-evidence phylogeny is conditioned on the rates of speciation, extinction, and fossilization, which are themselves conditioned on the sampling of lineages in the phylogeny (Stadler 2010). Early total-evidence phylogenies used unrealistic Yule (speciation only) or uniform priors on branch lengths (Pyron 2011; Ronquist et al. 2012), which recent authors have convincingly demonstrated yield excessively old dates (Beck and Lee 2014; Arcila et al. 2015). Recent improvements to the fossilized birth–death models seem to alleviate these biases in empirical data sets (Gavryushkina et al. 2014; Heath et al. 2014; Zhang et al. 2015), allowing for a more accurate representation of the evolutionary process, and true total-evidence phylogenetics incorporating morphology, molecules, and stratigraphy. Fossil sampling is also strongly nonrandom and should be modeled probabilistically, as well (Wagner and Marcot 2013; Holland 2016).

#### MODELING MORPHOLOGICAL CHARACTERS

These three points give an integrative picture of total-evidence analyses combining molecular and morphological data. However, relatively little attention has been paid recently to the dynamics of evolutionary substitution in discrete morphological characters

(Nylander et al. 2004; Klopstein et al. 2015). The Mk model (Lewis 2001) is analogous to the JC69 model (Jukes and Cantor 1969) for DNA-sequence data (Felsenstein 2004). As morphological matrices grow increasingly large, the probability that such a model adequately accounts for transitions among character states for different functional groups (Clarke and Middleton 2008; Mounce et al. 2016) seems very low. Presumably, few systematists would consider analyzing a large, multi-locus DNA-sequence matrix with a single JC69 model, as underfitting models for molecular data yields significant errors in estimating branch lengths and support values (Buckley and Cunningham 2002; Felsenstein 2004; Lemmon and Moriarty 2004).

For many characters, the plesiomorphic and apomorphic states occur at unequal frequencies through time, and have asymmetric rates of change. For instance, the morphological data set presented for Squamata by Gauthier et al. (2012) designated 0 as the hypothetical state of the lepidosauromorph ancestor, with 1 as the derived state. ~~Indeed, the final character in their matrix, 610, was oviparous (0) versus (1) viviparous reproduction.~~ While the ancestral state and potential for reversal in this character is controversial, it is certainly not symmetric and equally frequent (Pyron and Burbrink 2014; Wright et al. 2015). Thus, the assumption of the Mk model of equal forward and backward rates of transition is known to be violated, and it is difficult to imagine a more clear-cut case of model mis-specification for the data being analyzed.

Lewis (2001) reiterated that asymmetric rates could only be estimated for individual characters. Later authors proposed an approach where state frequencies were drawn from an overall prior distribution, which is implemented in MrBayes (Nylander et al. 2004). This approximates a model in which transition rates are asymmetric. Recently, this approach has been shown to improve phylogenetic resolution in many, but not all cases (Wright et al. 2015). However, this approach can also yield poor mixing and convergence, drastically increase computation time, and does not address the underlying epistemology of character-state labels. Instead, I propose a novel interpretation of state labels for modeling asymmetric rates.

Characters are often coded, or could be coded, with an implicit or explicit reference to ancestral or plesiomorphic states, derived from fossil observations or outgroup comparison (Hennig 1966; Farris 1982; Michevich 1982; Lipscomb 1992; Rieppel and Kearney 2002; Sereno 2007). I argue that we can actually exploit this coding bias to generate more meaningful evolutionary models. Along these lines, I propose that morphological state-labels are often non-arbitrary. Characters with nonarbitrary labels can be compared in a biologically meaningful way that allows for more complex model-based phylogenetic inference.

This logic could apply to multistate discrete or continuous characters, but I will restrict my discussion to binary characters defined explicitly such that 0 is the plesiomorphic state, and 1 is the apomorphic state

(Gauthier et al. 2012). Integrating over the underlying structure and function of the characters themselves, we can treat the labels 0 and 1 as representing “ancestral” and “derived,” and estimate meaningfully asymmetric transition rates and estimate unequal equilibrium frequencies for these states. From this base framework, we can extend the logic of simple models of DNA substitution to a morphological context with two character states. Variation in rates among sites can be handled using the traditional gamma-distributed rate-heterogeneity model. Modeling rate variation is complex; in some cases, adding more gamma categories or using a lognormal distribution may improve results (Harrison and Larsson 2015).

As extensions of the Mk model (Lewis 2001), I refer to these collectively as MkA (asymmetric) for the purposes of further discussion. In the binary case, the frequencies and rates of 0 and 1 are equivalent, and we can estimate asymmetric transitions by allowing the state frequencies  $\pi_0$  and  $\pi_1$  to vary, where  $\pi_0$  represents the forward rate and  $\pi_1$  the backward rate. Thus, we can incorporate the biological reality that forward and backward rates typically differ between plesiomorphic and apomorphic states for the types of morphological characters typically coded for phylogenetic inference. I suggest that most characters coded in morphological matrices do not reasonably have equal rates and frequencies, and are appropriately modeled thusly. In short, MkA is a F81-like model for binary characters that contains two parameters,  $\pi_0$  and  $\pi_1$ . These are the asymmetric forward and backward rates for transitions between the plesiomorphic state 0 and the apomorphic state 1, integrated across the individual characters.

Conveniently, this is already implemented in MrBayes as a F81-like model for presence/absence restriction-site data (Ronquist and Huelsenbeck 2003). It can be repurposed for MkA analysis of morphological data, by creating a separate partition for appropriately coded binary characters (data type = “restriction”), and setting the ascertainment bias to only parsimony-informative sites (coding = “informative”). Thus, an MkA total-evidence dating analysis might include a molecular partition (with appropriate models, e.g., GTR) and a multi-state morphological partition (Mkv), along with the binary partition (F81-like restriction = MkA).

Thus, the additional parameters estimated in MkA over Mkv are  $\pi_0$  and  $\pi_1$ , which are the stationary state frequencies of the ancestral and derived states. They are analogous to the base frequencies  $\pi_{A/T/G/C}$  in a molecular analysis. Because there are only two states, these are thus also equal to the rates of forward and backward change between states. They are fixed to 0.5 in Mkv, just as  $\pi_{A/T/G/C}$  are fixed to 0.25 in JC69, and estimated in other models like F81. The additional prior on these parameters is a flat Dirichlet distribution ( $\alpha=1$ ) giving equal probabilities for each combination of states ( $\sum \Pr[\pi_{0/1}] = 1$ ), as in most common analyses of DNA ( $\sum \Pr[\pi_{A,T,C,G}] = 1$ ). Thus, a single pair of  $\pi_{0/1}$  values is estimated for the binary partition, representing the overall forward and backward rate across the alignment.

A very similar, nonstationary model for binary characters was explored by Klopffstein et al. (2015), who allowed state frequencies at the root of the tree to vary from the constant frequencies across the descendant branches. Their approach uses the same F81-like model in MrBayes, adding a reversible-jump Markov sampler to move between stationary and non-stationary models. This approach can thus detect stasis or directional evolution in discrete morphological characters. They also noted that this logic could be used to estimate asymmetric transition rates, but did not explore this in their empirical example of hymenopterans. Their binary characters were coded as “absent”/“present,” and they thus focused on the frequency of character presence at the root versus equilibrium. Here, I extend this to a broader interpretation of plesiomorphy/apomorphy, which may be applicable in more cases.

Note that the assumption that the state labels represent plesiomorphy and apomorphy is not reflected in the models themselves, which do not assume ancestral states, but merely calculate instantaneous substitution probabilities among labeled states. Incorporating historical hypotheses of ancestral state to employ directional rates of change would require more complex models, but may be an interesting area for future research. As noted by Lewis (2001), these models make a number of assumptions that may strike many as being unrealistic. It is possible to envision a variety of other approaches to modeling morphological evolution that incorporate hypothesized ancestral states, connectivity among multistate characters, or other incidental parameters. This is in addition to other approaches using alternative priors on state frequencies and among-character rate variation (Harrison and Larsson 2015; Wright et al. 2015).

What benefits might we expect in an empirical case? In general, we might expect three major outcomes from employing ~~the~~ total-evidence and more accurate models for morphology. These would be (i) overturning strongly supported branches from Mkv and uncalibrated analyses (overcoming long-branch attraction or homoplasy), (ii) increasing precision and accuracy of branch-length estimates and support values (incorporating ~~ancestral character states~~), and (iii) increasing accuracy and precision for the placement of fragmentary fossils (reducing rogue placements from poorly optimized topologies). These might be expected from the combination of molecular and morphological data negating homoplasy, the introduction of an explicit time-scale from fossils for estimating clock rates and model parameters and limiting the probable topologies far in excess of what would be possible in an uncalibrated analysis, and more accurate models for morphological characters.

#### REVISITING THE SQUAMATE TREE OF LIFE

Here, I apply these principles to Squamata, the lizards, snakes, and amphisbaenians, a group with

AQ2



a contentious phylogenetic history (Losos et al. 2012; McMahan et al. 2015). Morphological and molecular data contain ambiguous, potentially conflicting signals that have created a difficult inference problem, with support for various topologies (Gauthier et al. 2012; Wiens et al. 2012). Recent authors have presented combined morphological and molecular analyses, not scaled to time, that they suggest represent “resolutions” of these problems (Wiens et al. 2010; Reeder et al. 2015). I show that even these integrated analyses may have been misled by the omission of time as a source of data for total evidence, and improper modeling of morphological characters.

The traditional morphological view of squamate phylogeny (Estes et al. 1988; Lee 2005b), illustrated by recent large-scale morphological analyses (Conrad 2008; Gauthier et al. 2012), supports a basal divergence between Iguania and Scleroglossa, which consists of Gekkota, Scincoidea, Lacertoidea, Anguimorpha, Serpentes, Dibamidae, and Amphisbaenia (groups *sensu* Jones et al. 2013). Typically, legless forms such as snakes, dibamids, and amphisbaenians group together in a single lineage, occasionally with legless members from other clades such as Gekkota, Scincoidea, and Anguimorpha. As the affinity of the legless gekkotans, skinks, and anguids is not in question, this result is presumably driven by homoplasy. There are also four fossil lineages of particular interest. One is *Huehuecuetzpalli*, one of the oldest squamate fossils, typically recovered as the sister taxon of all other squamates. Another is *Sineoamphisbaena*, which has been recovered in a variety of positions. Finally, the mosasaurs and polyglyphanodontians are sometimes recovered as sister lineages of Scleroglossa, nested deep therein, or various other alternatives (Lee 2005b).

In contrast, molecular data support gekkotans or dibamids as the earliest diverging squamate lineages, with successive divergences of Scincoidea, Lacertoidea (including Amphisbaenia), Anguimorpha, Iguania, and Serpentes (Wiens et al. 2012; Pyron et al. 2013). A major difference is thus the nested placement of Iguania, with molecular support for Toxicofera, a clade comprising Iguania, Anguimorpha, and Serpentes (Townsend et al. 2004; Fry et al. 2006). Legless forms are widely separated, nested within various other legged clades.

Several studies have attempted to combine morphological and molecular data sets in an uncalibrated framework to leverage the phylogenetic signal of both, overcome homoplasy, and provide a robust phylogenetic framework for placing fossil taxa (Lee 2005a, 2009; Wiens et al. 2010; Reeder et al. 2015). An early major study, based on more limited sampling of taxa and characters (Wiens et al. 2010), recovered higher level relationships similar to the molecular data alone, including Toxicofera. They also estimated *Huehuecuetzpalli* as the sister taxon of Iguania, mosasaurs nested in Anguimorpha, and polyglyphanodontids nested in Lacertoidea, which also contained Amphisbaenia. In their analysis, both morphological and molecular branches were rearranged

when data sets were combined, though the structure tended more toward the molecular tree, and many higher level nodes were weakly supported.

A more recent, large-scale study combined and expanded the morphological (Gauthier et al. 2012) and molecular (Wiens et al. 2012) “Squamate Tree of Life” data sets, also in an uncalibrated framework (Reeder et al. 2015). Again, they found a higher level structure more similar to the molecular tree (e.g., early-diverging gekkotans and dibamids, Iguania nested in Toxicofera, Amphisbaenia with Lacertoidea), but with strong support for most nodes. Mosasaurs were placed with snakes (Lee 2005a), and polyglyphanodontids were the sister taxon of Iguania in Toxicofera. Curiously, four taxa could not be placed strongly, and had to be removed from the analyses as “rogue” taxa. These were *Huehuecuetzpalli*, *Eichstaetisaurus*, *Sineoamphisbaena*, and an undescribed form, AMNH FR 21444, now known as *Norellius nyctisaurops* (Conrad and Norell 2006; Conrad and Daza 2015).

However, many researchers do not appear to be convinced of the validity of the molecular or combined results (Gauthier et al. 2012; Losos et al. 2012). There is morphological support for various topologies, including both early-diverging and nested Iguania (Reeder et al. 2015), and molecular support for both of those topologies, as well as an early-diverging Lacertoidea (McMahan et al. 2015). Furthermore, the length of the outgroup branch leading to *Sphenodon* may make character polarization difficult, potentially leading to problems identifying the proper rooting point for the ingroup (McMahan et al. 2015). Phylogenetically informative temporal evidence from the fossil record still have not been leveraged, which may alter topologies, branch lengths, and support for fragmentary fossils.

#### Morphological Data

All analyses were performed in MrBayes 3.2.5. I analyzed two morphological matrices concurrently. The first was presented by Gauthier et al. (2012), “GEA” hereafter. They presented 610 characters for 192 lepidosauromorph taxa: 3 rhynchocephalians including the extant outgroup *Sphenodon*, and 189 squamates, representing most major extant and extinct lineages. These 192 taxa represent 51 fossils and 141 extant lineages, concentrating on well-preserved fossil specimens and a diverse sampling of living clades. The matrix contains both ordered and unordered characters, which were specified in the analyses (see below). Conrad (2008) sampled 223 taxa, of which 129 were extinct and 94 were extant (“CON” hereafter). The extant sampling omits many living lineages (e.g., most advanced snakes are coded as “Neomacrostomata”), but includes denser fossil sampling in groups such as Anguimorpha, Mosasauria, and Scincoidea. This matrix consists of 363 unordered characters. Both score a wide variety of osteological and soft-tissue characters, often

taken from previous foundational analyses (e.g., [Estes et al. 1988](#)).

First, I analyzed each morphological data set separately in an uncalibrated analysis, using the Mkv model with variable coding and gamma-distributed rate heterogeneity ([Lewis 2001](#)). Second, I performed a calibrated analysis of each matrix, based on the morphological clock. I determined the time horizon of each fossil by conferring with experts (J. Conrad, personal communication), assessing the stratigraphic horizons of scored material, and consulting the Paleobiology Database (<http://www.paleodb.org/>). I enforced the fossil horizons as a uniform distribution on the tip age (Online Appendix I available on Dryad at <http://dx.doi.org/10.5061/dryad.dp3js>). Note that many tips are composites of multiple specimens across several time periods, and thus necessitate relatively broad tip-age priors.

For the root age, I used a uniform prior of 238.0–249.5 Ma, from a recent study presenting a stratigraphic and molecular meta-analysis of lepidosauromorph divergence times ([Jones et al. 2013](#)). Following [Zhang et al. \(2015\)](#), I used the fossilized birth–death prior on the branch lengths under diversified sampling. This is a sampled-ancestor process ([Stadler 2010](#); [Zhang et al. 2015](#)), and thus fossils can be direct ancestors of descendant branches. I calculated the approximate sampling proportion of extant lineages as 0.01 for CON (94/~9500 total species) and 0.015 for GEA (141 / 9500).

I followed [Zhang et al. \(2015\)](#) in placing broad priors on speciation ( $\exp[10]$ ), extinction ( $\text{beta}[1,1]$ ), and fossilization ( $\text{beta}[1,1]$ ). These priors are considered flat and uninformative, which is a cautious approach, given the sparse nature of the squamate fossil record. However, groups with denser, more detailed fossil series may be served by direct estimation of prior parameters such as turnover and sampling. Presumably, more accurate priors would place higher weight on nonzero extinction fractions and observed speciation rates.

For the relaxed clock rates, I used the independent gamma-rates (IGR) model ([Ronquist et al. 2012](#)), with a broad prior of  $\exp(10)$  on the IGR parameter describing rate variance through time. For the clock rate prior, since all morphological characters are variable, we can assume *a priori* that each one changes at least once across the timescale of the tree. Thus, I used 1/243.75 Ma (the mean of the root-age prior) = 0.004103 substitutions per million years. In lognormal space, this is a mean of  $-5.496143$ , for which I gave a large standard deviation as the exponent of the mean,  $\exp(0.004103) = 1.004111$ . This gives a broad prior density of 0.0005–0.03 subst./My, which should accommodate both the morphological and molecular partitions.

The calibrated and uncalibrated analyses allow us to estimate the morphological clock, and evaluate the effect of imposing a timescale on topology and support values in the total-evidence framework for the morphological partition alone. I ran 4 runs of 4 chains for at least 25 million generations, sampled every 10,000th, with the first 25% discarded as burnin (e.g., 18.75 million

post-burnin generations). I assumed convergence when the estimated sample size (ESS) reached  $>100$  for all parameters ([Drummond and Rambaut 2007](#)). These conditions were used for all subsequent analyses. Some analyses had to be run longer, up to 50 million generations.

I also analyzed the GEA matrix using the MkA approach in three conformations. The matrix contains 374 binary characters. The authors explicitly note that binary characters were coded with respect to a hypothetical lepidosauromorph ancestor ([Gauthier et al. 2012](#)), allowing the MkA logic to be applied to this partition. The remaining partitions received ordinary Mkv+ $\Gamma$  models ([Lewis 2001](#)). Using the conditions described above, I analyzed the morphological alone (calibrated using the fossilized birth–death prior), the morphological and molecular data combined in an uncalibrated analysis, and a total-evidence analysis of the morphological and molecular data using the fossilized birth–death prior.

Applying the F81-like restriction-site model with parsimony-informative ascertainment bias correction ([Klopfstein et al. 2015](#)), I was able to estimate asymmetric rates for forward and backward transitions under the MkA logic. To compare models, I used the stepping-stone approach ([Xie et al. 2011](#)) to test the fit of MkA over Mkv. Because these analyses are computationally intense (~50 times longer than normal), I only compared the uncalibrated analysis of the GEA matrix alone, using Mkv and MkA. For each, I ran a single chain for 2.6 million generations, for a total of 50 stepping-stone samples, and compared the estimated marginal likelihoods using  $\log(\text{Bayes factors})$ . If the increase in model fit from MkA is significant in this simplest case, we can assume MkA is an appropriate model for more complex total-evidence analyses.

#### Molecular Data

For the extant lineages in the morphological data sets, I pruned and modified an existing molecular data set ([Pyron et al. 2013](#)) to match those taxa for a subset of loci. I included 12S/16S and cytochrome *b* for mitochondrial loci, and BDNF, CMOS, and RAG1 for nuclear loci. These 6 genes were sufficient to ensure that each of the 141 species (or a congener) in the GEA matrix were represented by at least 1 locus. For the CON matrix, I added the mitochondrial gene ND2, as this was the only locus sampled for many of the extant taxa.

As noted above, more extensive data sets of at least 40–50 loci could be assembled for most of these species ([Wiens et al. 2012](#); [Reeder et al. 2015](#)). However, as noted by those authors, the sheer size of the data sets presents significant issues of computational tractability and convergence, given the large number of parameters. Furthermore, smaller molecular data sets are already known to yield essentially identical topological results ([Townsend et al. 2004](#)). Additionally, data sets of just a few loci have already been shown

AQ6

to yield essentially identical divergence-time estimates for squamates (Mulcahy et al. 2012). Finally, even if more loci are added, several lineages (e.g., *Anomochilus*, *Xenophidion*) would still only be represented by one or a few loci, with massive amounts of missing data.

Instead, I used this representative molecular data set, determining the optimal partitioning and parameterization strategy with PartitionFinder (Lanfear et al. 2012). The two matrices are similar but not identical, and should represent the “typical” molecular signal. First, I analyzed each molecular matrix without temporal calibrations, approximating previous studies (Townsend et al. 2004; Wiens et al. 2012; Pyron et al. 2013). Second, I estimated a calibrated tree from each matrix, using the same analytical conditions described above for the morphological partitions, the only difference being a lack of noncontemporaneous fossils. Thus, the only information present for dating nodes was the prior on the root age and the clock rates. This allows us to observe the difference between the signal derived from calibrated and uncalibrated molecular analyses, and estimate the molecular clock.

Finally, I paired each morphological matrix with its taxonomically matching molecular matrix, and estimated uncalibrated and total-evidence-dated phylogenies, using the parameters described above. Thus, we can compare the effects of imposing a timescale on the morphological data alone, the molecular data alone, and the combined morphological and molecular data. Furthermore, we can compare these effects between two different sampling strategies of characters and taxa, to evaluate whether lineages change placement when scored in different matrices. If any large variations occur, it will be difficult to determine if either is correct *per se*, but this will at least provide a starting point for future analyses to investigate those lineages in detail.

#### Effects of Parameterization

Above, I suggested that improvements from time calibration (i.e., total evidence) and the use of MkA or similar approaches might be marked by (i) overturned branches, (ii) increased node support, and (iii) increased support for “rogue” taxa. While an individual comparison of placements for all lineages in each data set is beyond the scope of this article, we can make some preliminary qualitative and quantitative assessments of these effects. We can evaluate major topological changes, increases in support and precision of node ages, and changes in topology and support for fragmentary fossils in particular, for calibrated and uncalibrated pairs, and for MkV versus MkA. I evaluate this only for analyses including morphological data, as the effects are seemingly minor for molecular analyses that lack fossils.

To evaluate the effects on support, I tested for a significant difference in support values for nodes shared between calibrated and noncalibrated analyses, using a Wilcoxon Rank-Sum test. I then regressed the

differences in support values against the support from the uncalibrated analysis, where a significantly negative slope indicates that poorly supported nodes in the uncalibrated analysis are supported more strongly in the calibrated analysis. I repeated these tests comparing the MkA analyses to their MkV counterparts.

I evaluated rogue taxa by running the RogueNaRok algorithm (Aberer et al. 2013) for 100 randomly selected trees from the posterior of each analysis. This yields taxa flagged as rogues, and their rogue scores, indicating the increase in support gained from their removal. I used a minimum threshold of 0.5 (e.g., removing the taxon results in a single bipartition supported at 50% being added to the majority-rule consensus). This allows me to compare uncalibrated and calibrated and MkV and MkA analyses to determine if rogue scores were reduced. Finally, I determined if the estimated ages and proportional confidence intervals (95% date range divided by the mean age) were significantly different for the MkV and MkA combined data, calibrated analyses. We would not necessarily expect mean ages to be different, but smaller proportional confidence intervals would indicate higher precision of MkA over MkV.

## RESULTS

### Morphological Data

Unsurprisingly, both morphological matrices yield results similar to previous analyses and morphological understandings of squamate phylogeny (Estes et al. 1988; Conrad 2008; Gauthier et al. 2012). In both analyses, the basal divergence in Squamata occurs between Iguania and Scleroglossa, which are both strongly supported. Overall, support is weak to moderate in both analyses, and the uncalibrated morphological analyses do not, on their own, offer a well-resolved picture of squamate evolution (Fig. 1). All trees were summarized as the Maximum Clade Credibility Tree with Common Ancestor Heights in TreeAnnotator (Drummond and Rambaut 2007). The full versions of all phylogenies, including taxon labels, support values, and estimated ages and confidence intervals, are available as Supplementary Material on Dryad.

In the CON analysis, the fossil *Huehuetzcpalli* is the sister lineage of Scleroglossa. Within Scleroglossa, there are successive divergences of Gekkota, Scincoidea (part) + Lacertoidea, Scincoidea (part) + the legless clade, and Anguimorpha. There is a primarily legless clade consisting of Scincoidea (part), Dibamidae, Amphisbaenia, and Serpentes. Scincoidea is paraphyletic; some of the legged and legless members group with the legless clade, while other legged members group with Lacertoidea and Anguimorpha. Polyglyphanodontidae is nested in Lacertoidea, while Mosasauria is nested in Anguimorpha. The fossils *Norellius*, *Eichstaettisaurus*, and *Sineoamphisbaena* are weakly placed in the CON analysis, the first two with Gekkota, and the latter within polyglyphanodontids.





FIGURE 1. Consensus topologies for the uncalibrated Mkv analysis of the CON matrix (a), the calibrated Mkv analysis of the CON matrix (b), the uncalibrated Mkv analysis of the GEA matrix (c), and the calibrated Mkv analysis of the GEA matrix (d).

The calibrated analysis of the CON matrix yields similar results to the uncalibrated analysis, with a few important differences. The estimated ages are somewhat inconsistent with recent consensus analyses (Jones et al. 2013), both older and younger for some clades (Table 1). The fossil *Huehuecuetzpalli* is the sister lineage of Iguania. Within Scleroglossa, Gekkota is the earliest diverging lineage. Importantly, the legless clade is partially broken up in the total-evidence analysis. There is a large clade consisting of a paraphyletic Scincoidea (including the legless skinks), Lacertoidea, and Polyglyphanodontidae, which is the sister lineage

of the remaining scleroglossans. A legless clade consisting of Dibamidae + Amphisbaenia is weakly nested in Serpentes. This clade is the sister lineage of Anguimorpha, which contains Mosasauria. The fossils *Norellius* and *Eichstaettisaurus* remain weakly placed with Gekkota, and *Sineoamphisbaena* remains weakly nested in Polyglyphanodontidae.

In the uncalibrated GEA analysis, *Huehuecuetzpalli* is strongly supported as the sister lineage of Squamata, and polyglyphanodontids and mosasaurs are the successive sister lineages of Scleroglossa. Within Scleroglossa, there are successive divergences of Gekkota,

TABLE 1. Estimated dates from Jones et al. (2013) as a recent stratigraphic and molecular reference, and from the total-evidence analyses presented here

Node	Jones et al. (2013)	CON DNA	GEA DNA	CON morph.	CON combined
Lepidosauria	242 (238–249.5)	243.7 (238.3–249.2)	243.8 (238.5–249.4)	240.5 (238.0–245.4)	240.9 (238.0–246.4)
Squamata	193 (176–213.2)	216 (185.2–244)	216.2 (188–244.5)	200.2 (180.8–221.7)	205.9 (182.7–229.6)
Gekkota	76.2 (52.4–101)	151 (117.6–187.2)	126.8 (99.4–156.9)	41.6 (24.5–60.8)	68.4 (50.4–85.5)
Scincoidea	137.6 (107.3–168.7)	156.4 (121.3–191.8)	165.2 (135.7–196.8)	—	130.5 (113.2–149.4)
Lacertoidea	150 (116.4–190.7)	169 (135–202.7)	179.7 (151.8–208.5)	—	131.1 (114.7–147.2)
Serpentes	109.6 (81.1–137)	128.3 (95.5–160.8)	140 (110.6–167.2)	—	119.1 (110.0–129.0)
Anguimorpha	129.5 (128.1–134.2)	129.1 (98.8–158.9)	121.6 (93.3–149.6)	136.2 (126.2–146.2)	138.8 (130.5–148.2)
Iguania	135.8 (116.7–152)	162.9 (132.5–194.1)	168.8 (138.6–197.3)	103.5 (93.0–115.3)	124.1 (111.5–136.7)

Node	GEA morph.	GEA combined	GEA morph. MkA	GEA com. MkA
Lepidosauria	243.9 (238.6–249.5)	244.3 (238.8–249.5)	244.2 (238.7–249.5)	244.5 (239.0–249.5)
Squamata	199.3 (179.9–219.5)	190.3 (172.6–208.5)	199.6 (179.4–220.4)	186.8 (172.3–202.7)
Gekkota	73.7 (48.5–98.1)	89.4 (70.2–108.2)	70.9 (47.8–95.0)	89.1 (72.0–103.9)
Scincoidea	134.4 (112.9–155.5)	147.0 (131.8–161.9)	136.0 (114.7–157.7)	146.9 (131.6–161.5)
Lacertoidea	—	156.1 (138.6–172.8)	—	151.4 (136.1–164.9)
Serpentes	117.3 (103.8–130.5)	123.3 (118.7–145.0)	118.0 (104.4–132.4)	121.8 (118.4–142.4)
Anguimorpha	—	114.3 (99.5–129.4)	—	113.4 (101.4–126.1)
Iguania	129.4 (109.9–149.6)	133.0 (117.1–150.2)	127.0 (108.6–147.5)	129.0 (115.3–141.4)

Notes: Ages are the mean and 95% HPD for the crown groups of extant taxa. Nonindicated dates (—) mean that the clade was not recovered as monophyletic in that analysis.

Anguimorpha (part), Lacertoidea, and Scincoidea. Scincoidea is paraphyletic with respect to a legless clade consisting of some legless skinks, Dibamidae + Amphisbaenia, *Anniella* (an anguimorph), and Serpentes. The fossils *Nyctisaurops* and *Eichstaettisaurus* are strongly placed with Gekkota in the GEA analysis, though *Sineoamphisbaena* is again weakly nested in polyglyphanodontids. This does not differ significantly from previous results (Gauthier et al. 2012).

For the calibrated analysis based on the morphological clock, the GEA analysis also results in a similar topology to the uncalibrated analysis, with several important differences, and remarkably congruent dates with recent stratigraphic and molecular meta-analyses (Jones et al. 2013; Table 1). Three major differences are observed from the uncalibrated analysis, highlighting the importance of the total-evidence approach. First, *Sineoamphisbaena* moves from Polyglyphanodontidae to become the sister lineage of the legless clade. Second, Mosasauria and Polyglyphanodontidae form a weakly supported clade as the sister lineage to Scleroglossa, rather than successive sister lineages. Third, Scincoidea is monophyletic (including the legless skinks), and moves to the sister lineage of Lacertoidea (excluding Amphisbaenia). Thus, the legless clade is partially broken up by the addition of temporal data.

#### Molecular Data

The molecular trees and dates are highly similar to essentially all recent estimates (Townsend et al. 2004; Wiens et al. 2012; Jones et al. 2013; Pyron et al. 2013), and most relationships are strongly supported (Fig. 2, Table 1). As in most studies, I find strong support

for Dibamidae or Gekkota as the earliest diverging squamate lineages, though weak support for their exact placements with respect to each other. All limbless non-snakes (e.g., skinks, anguids, amphisbaenians) are placed in their traditional lineages, and do not form a clade with snakes. Toxicofera is strongly supported, with snakes as the sister lineage to Iguania + Anguimorpha, which is weakly supported by both matrices.

#### Combined Analyses

For the combined analysis using the CON matrix and corresponding molecular sampling, the uncalibrated runs yield a consensus topology that is poorly supported, and notably divergent from either of the underlying data partitions, particularly in supporting an apparently erroneous legless clade at the same time as a nested Iguania (Fig. 3). There are successive divergences of Gekkota, Dibamidae, and Scincoidea. Next is a clade consisting of Lacertoidea (including Polyglyphanodontidae) and Serpentes + Amphisbaenia. The fossil *Huehucuetzpalli* is the sister lineage of Iguania, and this clade is the sister lineage of Anguimorpha (including Mosasauria).

The calibrated CON analysis yields a fairly similar topology. The only major difference is that Serpentes becomes the sister lineage of Iguania + Anguimorpha, breaking up the legless clade and forming Toxicofera. Lacertoidea thus includes Polyglyphanodontidae and Amphisbaenia. Overall, support for the calibrated analysis is weak for many nodes. RogueNaRok identifies four major (score >0.5) rogues: *Colpodontosaurus*, *Palaeosaniwa*, *Ardeosaurus*, and *Lanthanotus*. Pruning

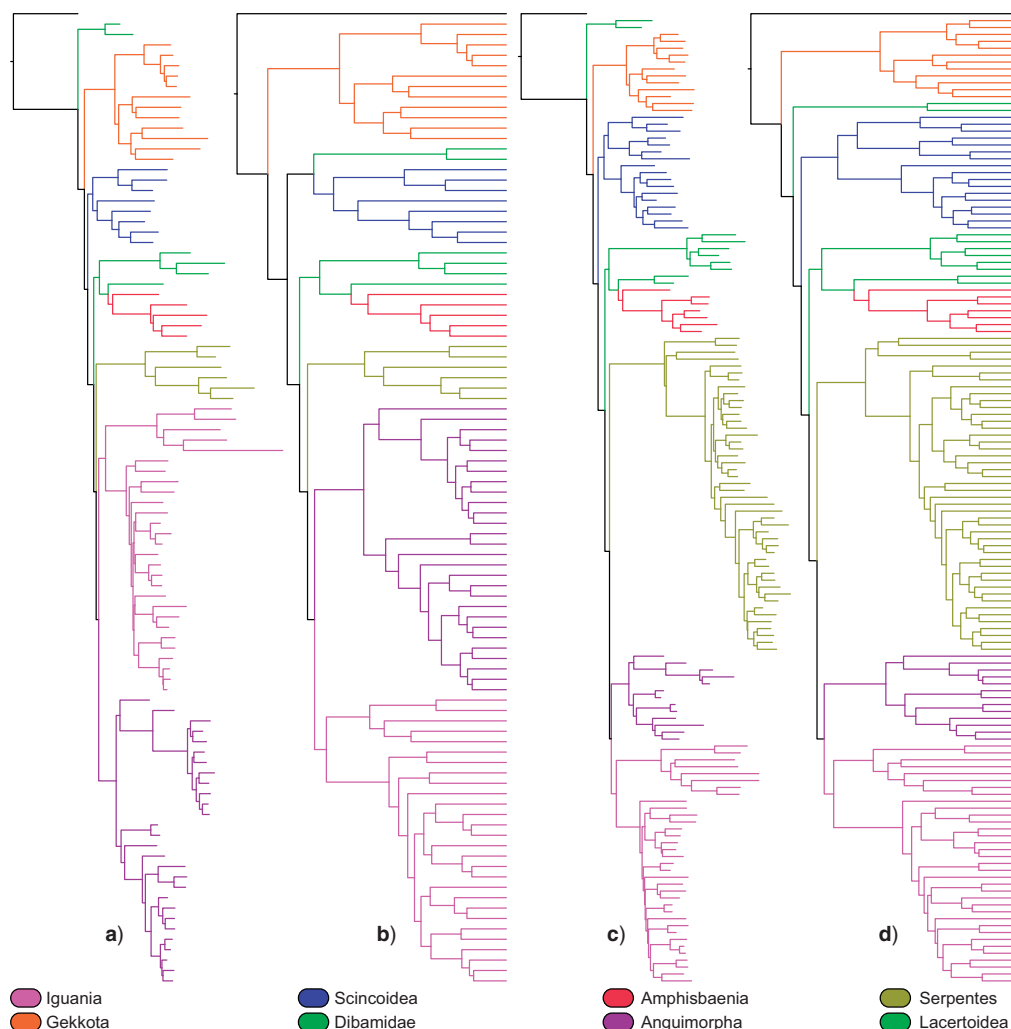


FIGURE 2. Consensus topologies for the uncalibrated analysis of the CON-congruent molecular matrix (a), the calibrated analysis of the CON-congruent molecular matrix (b), the uncalibrated analysis of the GEA-congruent molecular matrix (c), and the calibrated analysis of the GEA-congruent matrix (d).

them from the posterior distribution yields increased support for many nodes (Fig. 4), suggesting that their fragmentary nature precludes strong placement, at least without more sophisticated models like MkA. Interestingly, the four rogues identified by previous authors in the GEA matrix, *Eichstaettisaurus*, *Huehucuetzpalli*, *Norellius*, and *Sineoamphisbaena* (Reeder et al. 2015) are not rogue in the CON matrix.

For the analysis using the GEA matrix and corresponding molecular sampling, the uncalibrated

analysis yields a consensus topology that is, like the CON analysis, poorly supported and divergent from either the molecular or morphological hypotheses. Gekkota is the earliest diverging squamate lineage (including *Eichstaettisaurus* and *Norellius*), followed by Scincoidea. Lacertoidea is the sister lineage to a legless clade comprising *Sineoamphisbaena*, Amphisbaenia, and Dibamidae + Serpentes. This group (Lacertoidea + legless clade) is the sister lineage of a clade including Anguimorpha + Iguania. Finally, *Huehucuetzpalli*,

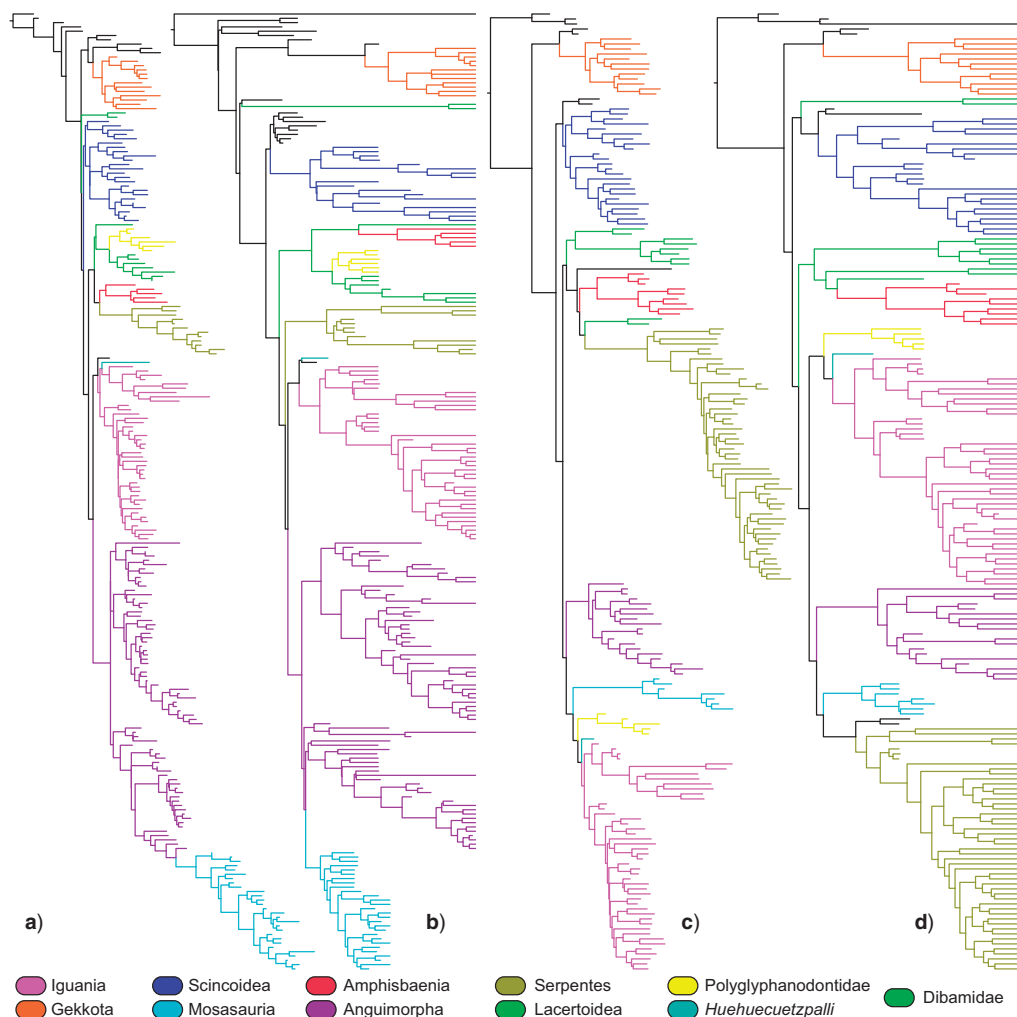


FIGURE 3. Consensus topologies, using Mkv for the morphological data and the optimal partitioning strategy for the molecular data, for the uncalibrated, combined-data analysis of the CON matrix and CON-congruent molecular matrix (a), the calibrated, combined-data analysis of the CON matrix and CON-congruent molecular matrix (b), the uncalibrated, combined-data analysis of the GEA matrix and GEA-congruent molecular matrix (c), and the calibrated, combined-data analysis of the GEA matrix and GEA-congruent matrix (d).

Polyglyphanodontidae, and Mosasauria are the successive sister lineages of Iguania.

In keeping with the potential outcomes described above, the calibrated topology more closely resembles recent molecular and uncalibrated combined analyses (Wiens et al. 2012; Pyron et al. 2013; Reeder et al. 2015), but with clear contributions from the fossil-tip dates. Gekkota (with *Norellius* and *Eichstaettisaurus*) is the earliest diverging squamate lineage, followed by successive divergences of

Dibamidae + Scincoidea, Lacertoidea (including Amphisbaenia + *Sineoamphisbaena*), Iguania, and Serpentes + Anguimorpha. The fossil lineages *Huehuecuetzpalli* and Polyglyphanodontidae are the successive sister lineages of Iguania, and mosasaurs are placed with snakes (Fig. 3). However, support for the backbone is relatively low, apparently driven by the rogue placement of *Sineoamphisbaena* as noted by previous authors (Reeder et al. 2015).

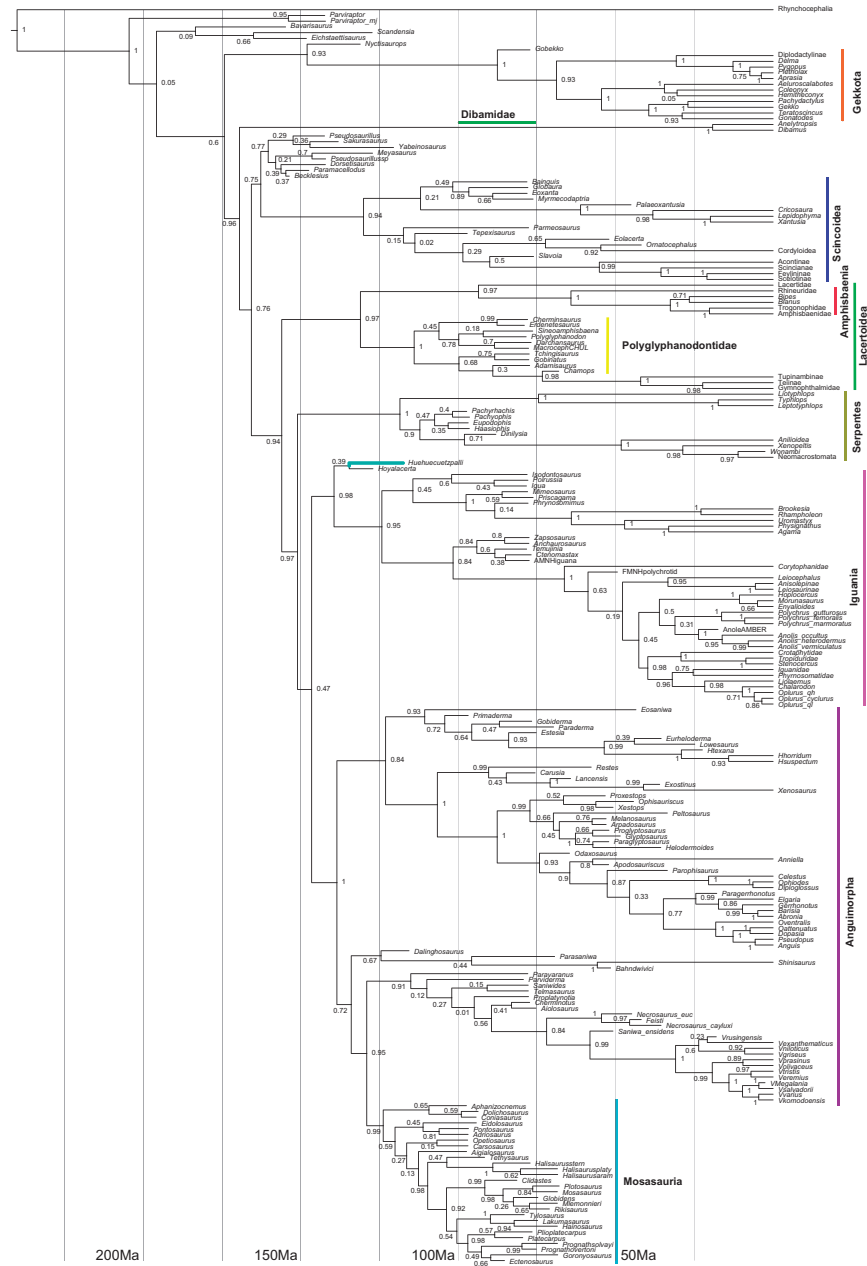


FIGURE 4. Consensus topology for the calibrated, combined-data analysis of the CON matrix and CON-congruent molecular matrix, with the four highest-scoring rogue taxa (*Colpodontosaurus*, *Palaeosaniwa*, *Ardeosaurus*, and *Lanthanotus*) removed. Node support values are posterior probabilities. I have preserved the taxon names (and occasional minor misspellings) of Conrad (2008), for easy reference with his previous work; “*Nyctisaurops*” is *Norellius nyctisaurops* (AMNH FR 21444). This is a pruned version of Fig. 3b.



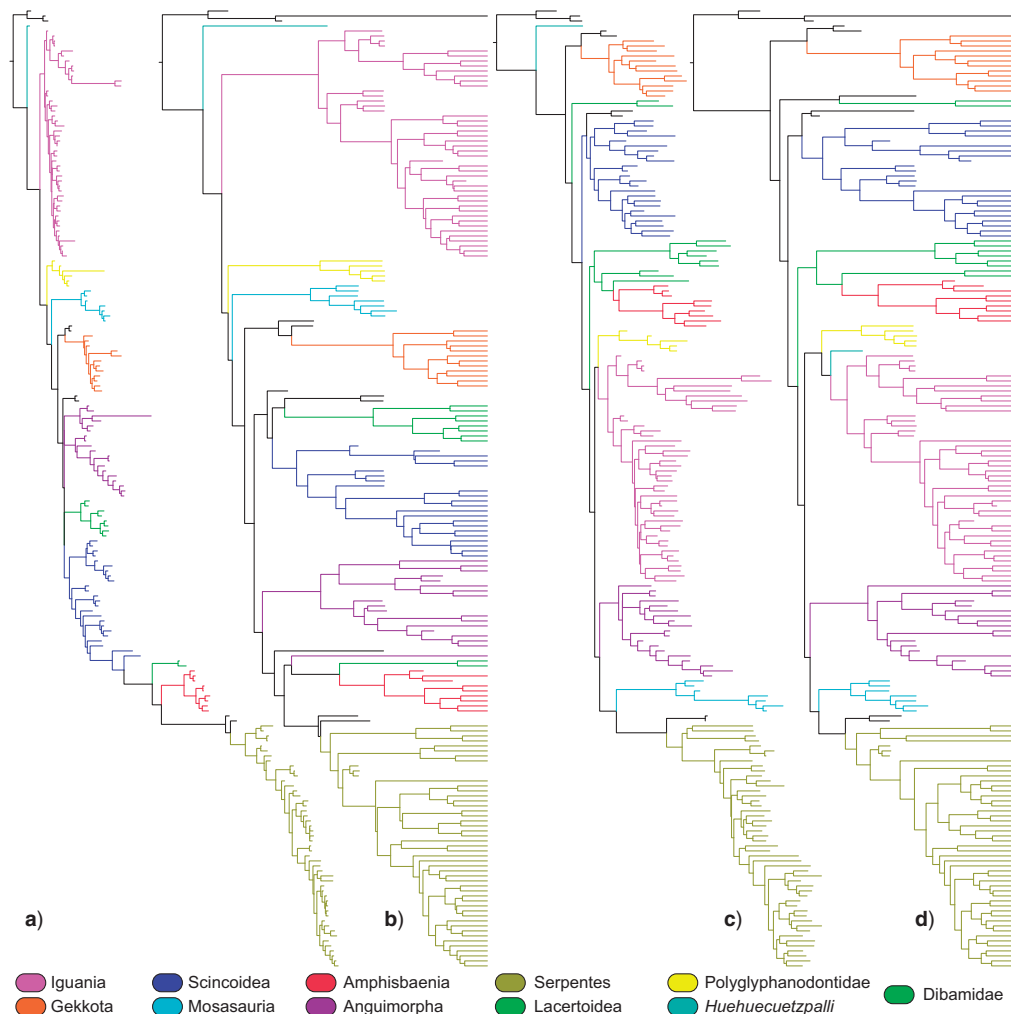


FIGURE 5. Consensus topologies using MkA for the binary characters and the optimal partitioning strategy for the molecular data, for the uncalibrated analysis of the GEA matrix (a), the calibrated analysis of the GEA matrix (b), the uncalibrated, combined data analysis of the GEA matrix and GEA-congruent molecular matrix (c), and the calibrated, combined data analysis of the GEA matrix and GEA-congruent molecular matrix (d).

### MkA

Applying the MkA logic to the GEA matrix, with and without morphological data and with and without time calibration, yields similarly complex results (Fig. 5). The estimated marginal likelihood of the MkV model using the stepping-stone method was  $-22929.67$ , and MkA was  $-22634.51$ , giving a Bayes factor difference of  $295.16$ , with  $>10$  usually considered “strong support” (Kass and Raftery 1995). Thus, I consider MkA to be

the best-fit model generally, for analyses using the GEA matrix. The estimated transition rates from the MkA models are  $\pi_0 \sim 0.7$  and  $\pi_1 \sim 0.3$  for all analyses, including morphology alone and combined data, for both uncalibrated and calibrated runs. Thus, reversals to the plesiomorphic state are overall about half as frequent as forward transitions to the derived state.

For the uncalibrated morphological matrix alone, the topology is similar to the MkV analysis (described above), with two main differences. First, *Anniella* is

placed (presumably correctly) in Anguimorpha, rather than in the legless clade. Second, within the legless clade (nested in Scincoidea, with legless skinks as the earliest diverging lineages), Dibamidae is the sister lineage of Amphisbaenia + Serpentes, rather than Dibamidae + Amphisbaenia forming the sister lineage of Serpentes. For the calibrated analysis, the results are again similar, except that mosasaurs and polyglyphanodontids are the successive sister lineages of Scleroglossa, rather than forming a single clade as the sister lineage of Scleroglossa.

The uncalibrated, combined data MkA analysis of the GEA matrix is relatively similar to the molecular results and previous analyses (Reeder et al. 2015). The earliest diverging squamate lineage is *Huehuecuetzpalli*, followed by Gekkota (including *Eichstaettisaurus* and *Norellius*), Dibamidae, Scincoidea, Lacertoidea (including Amphisbaenia + *Sineoamphisbaena*), Iguania + Polyglyphanodontidae, Anguimorpha, and Serpentes + Mosasauria. Compared to the uncalibrated MkV analysis, the uncalibrated MkA model breaks up the legless clade, places mosasaurs with snakes, amphisbaenians with lacertids, and dibamids and *Huehuecuetzpalli* in an early-diverging position. Thus, the uncalibrated MkA analysis appears to be more accurately resolved than the uncalibrated MkV analysis described above.

The calibrated MkA analysis is essentially identical to the uncalibrated MkA analysis, with the primary differences being that *Huehuecuetzpalli* moves to become the sister lineage of Iguania, and *Sineoamphisbaena* moves to become the sister lineage of Dibamidae. Interestingly, there are no taxa flagged as “rogues” by RogueNaRok. This is contrary to all other analyses, and previous results using these data sets (Reeder et al. 2015). I treat this result as my best estimate of squamate phylogeny (Fig. 6).

#### Rogue Taxa

Patterns of rogue taxa are complex in the CON-based analyses, with 43 species flagged by RogueNaRok in at least one analysis. Of these, 15 taxa are flagged in at least two analyses, providing a basis for comparison (Table 2). Calibrating the morphological analysis decreases rogue scores for 5 taxa and increases them for 10. Calibrating the combined analysis decreases scores for 6 taxa, increases them for 7, and leaves 2 unchanged. Adding molecular data in uncalibrated analyses decreases scores for 5 taxa, increases them for 6, and leaves 4 unchanged. Adding molecular data in calibrated analyses decreases scores for 6, increases them for 7, and leaves 2 unchanged. Thus, for the CON matrix, the effects of total-evidence dating on rogue taxa are ambiguous. I suggest that this is due to the shorter matrix (363 characters) and larger number of fragmentary fossils, so I do not discuss these patterns in detail here beyond removing the highest-scoring rogues (Fig. 4). This matrix is being expanded (J. Conrad, personal communication), and support for these problematic taxa may increase in future studies.

Rogue taxa are limited in the GEA-based analyses (Table 3). While 13 species had nonzero scores in at least one analysis, only 5 were flagged in at least two, giving a basis for comparison. Note that *Norellius* and *Eichstaettisaurus* are not among these, in contrast to Reeder et al. (2015). For *Sineoamphisbaena*, both calibration and MkA reduce rogue scores. For *Huehuecuetzpalli*, MkA actually increases rogue scores for the combined analyses, but calibration reduces them. However, neither taxon is strongly placed in the best estimate of the GEA-based phylogeny (Fig. 6). Overall, both calibration and MkA reduce rogue-taxon scores in a majority of cases (Table 3).

#### Effects of Parameterization

Introducing a timescale clearly exerts a strong influence on topology, often overturning major branches. Qualitatively, the major effect is partially breaking up the legless clade, returning legless skinks to their correct group, and altering the placement of snakes and amphisbaenians. Other fossil lineages move between analyses, but I do not address these in detail. Support in calibrated analyses is significantly higher only for the CON morphological matrix and the GEA combined data analysis, and none of the other CON- or GEA-based analyses. However, the slope of the difference is significantly negative for all tested pairs ( $P < 0.05$ ), indicating that weakly supported nodes in uncalibrated analyses are generally more strongly supported in calibrated analyses in all cases.

For the MkV versus MkA comparisons, the difference in support is significant for the combined data analyses; the calibrated MkA analysis has significantly higher support than the calibrated MkV analysis. None of the other comparisons are significant. The slope is also significantly negative for all comparisons ( $P < 0.05$ ), indicating that MkA increases support over MkV for more weakly supported nodes in all cases. This is in addition to the increase over calibration alone. Thus, both calibration and MkA almost always increase support.

Similarly, the proportional confidence intervals are significantly narrower in the MkA tree ( $P < 0.05$ ), indicating greater precision in estimated node ages. However, the increase in precision does not vary with node age; precision in ages increases uniformly across the phylogeny. The estimated node ages are also significantly younger in the MkA tree, though only by 0.75 Ma on average, with a maximum 4 Ma difference. The age differences exhibit a small but significant negative slope ( $P < 0.05$ ), indicating that older nodes are typically younger in the MkA analysis. Thus, node support and precision in estimated node-ages increases uniformly in the MkA analysis, and rogue scores decrease for both extinct and extant taxa. Therefore, all three predicted positive effects (increased topological resolution, increased support and precision for branches, and decreased fossil instability) are observed from the addition of an explicit total-evidence timescale, and the use of the MkA model for polarized, binary characters.

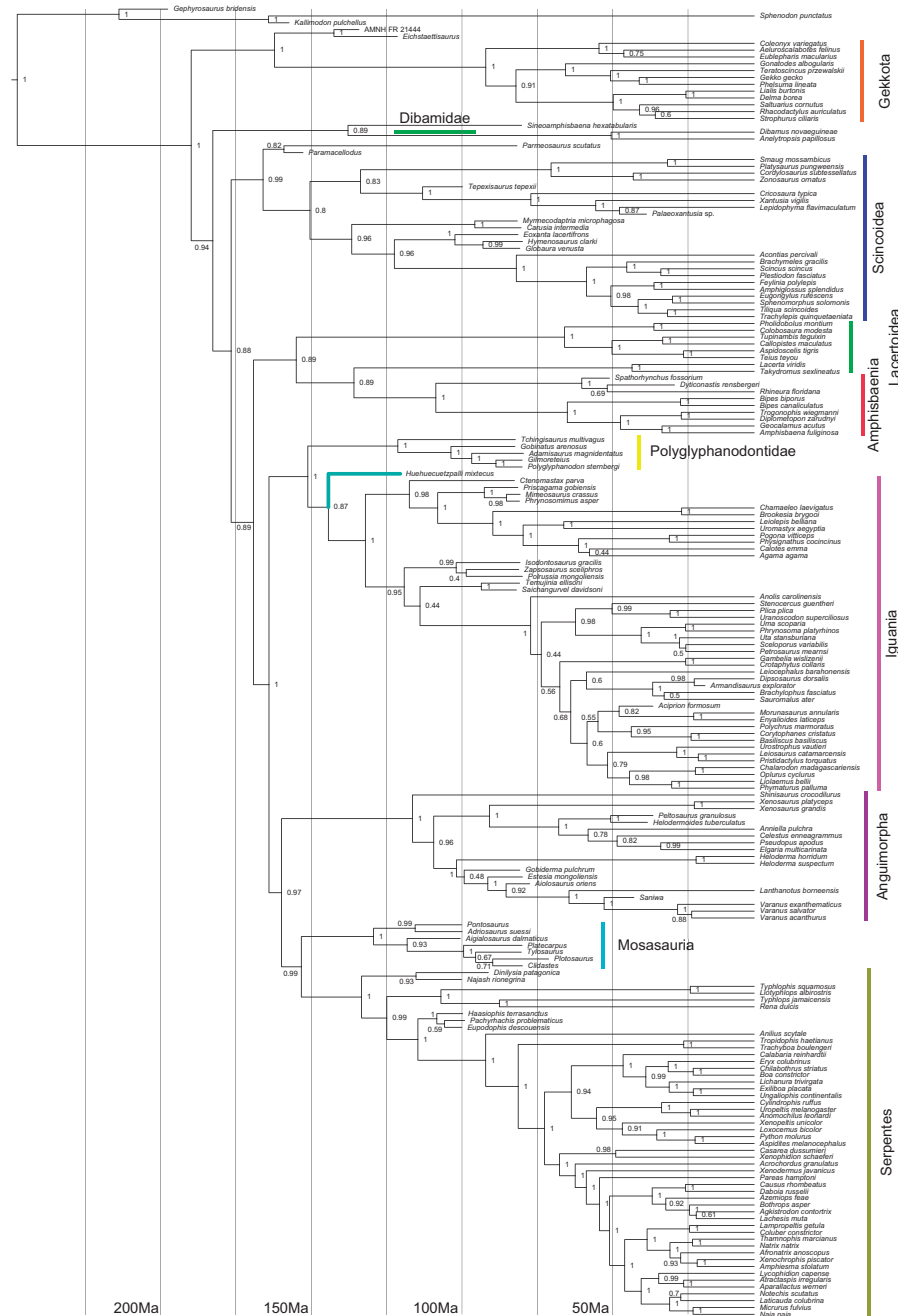


FIGURE 6. Consensus topology for the calibrated, combined data analysis of the GEA matrix, and GEA-congruent molecular matrix using the MkA model for the binary characters. Node support values are posterior probabilities. This is the full version of Fig. 5d.

TABLE 2. Rogue scores for CON taxa registering nonzero values for at least two comparable analyses

Taxon	Morph Uncal	Cal	All Uncal	Cal
<i>Aiolosaurus</i>	0.25	—	—	0.15
<i>Carsosaurus</i>	0.65	0.14	—	—
<i>Chamops</i>	—	0.35	0.5	—
<i>Colpodontosaurus</i>	—	1.53	0.01	2.35
<i>Coniasaurus</i>	0.09	0.77	0.09	0.24
<i>Dorsetisaurus</i>	0.62	—	0.25	0.03
<i>Eidolosaurus</i>	—	0.69	0.85	0.01
<i>Eolacerta</i>	—	0.16	—	0.29
<i>Eosaniwa</i>	0.21	0.29	1.5	—
<i>Huehucuetzpalli</i>	0.12	—	0.23	—
<i>Pachyophis</i>	0.48	0.54	—	—
<i>Palaeosaniwa</i>	—	0.67	0.21	1.09
<i>Paravaranus</i>	—	0.31	—	0.37
<i>Parneosaurus</i>	—	0.01	—	0.32
<i>Xestops</i>	0.47	—	0.2	—

Note: Other taxa not shown had low rogue scores (<0.5) in only one analysis, but this is not informative for comparison.

TABLE 3. Rogue scores for GEA taxa registering nonzero values for at least two comparable analyses

Mkv					
Taxa	Morph	uncal	Morph	cal	All uncal All cal
<i>Anniella pulchra</i>	0.13	—	1.85	—	—
<i>Atractaspis irregularis</i>	0.41	—	0.15	—	—
<i>Huehucuetzpalli mixtecus</i>	—	—	—	0.29	—
<i>Phrynosoma platyrhinos</i>	—	—	—	—	—
<i>Sineoamphisbaena hexatabularis</i>	2.52	—	—	0.9	0.76

MkA					
Taxa	Morph	uncal	Morph	cal	All uncal All cal
<i>A. pulchra</i>	4.16	—	1.02	—	—
<i>A. irregularis</i>	—	—	0.79	—	—
<i>H. mixtecus</i>	—	—	—	0.94	—
<i>P. platyrhinos</i>	0.07	—	0.15	—	—
<i>S. hexatabularis</i>	1.04	—	—	0.44	—

## DISCUSSION

### Total Evidence and Morphology

The necessity of stratigraphic congruence in estimated phylogenies is evident from first principles (Huelsenbeck 1994; Benton et al. 1999), and is the subject of a large paleobiological literature (see Smith 1998; Fisher 2008). However, many recent studies have ignored stratigraphic data when placing fossil taxa (e.g., Conrad 2008; Gauthier et al. 2012; Wiens et al. 2010; and Reeder et al. 2015 for Squamata). While total-evidence dating is stratigraphically congruent by definition, some authors have reported excessively old dates from total-evidence studies (Beck and Lee 2014; Arcila et al. 2015). This bias seems to have been caused by improper priors, and mostly solved by the fossilized birth–death process (Zhang et al. 2015).

Reassuringly, the total-evidence dates estimated here are remarkably similar to recent consensus estimates (Jones et al. 2013) from stratigraphic and molecular data (Table 1). As I demonstrate here both qualitatively and quantitatively, adding a temporal dimension induces three desirable effects: (i) overturning apparently artifactual branches (e.g., partially breaking up the legless clade), (ii) increasing node support (e.g., significant increases for calibrated and MkA analyses), and (iii) reducing “rogue” placements (e.g., increased support for *Eichstaettisaurus*, *Huehucuetzpalli*, *Norellius*, and *Sineoamphisbaena*), confirming earlier studies showing positive effects of temporal calibration (Wagner 1998).

Similar to omitting stratigraphic data, inadequate models for morphology may hamper total-evidence dating if they under-fit the substitution process, and cannot accurately estimate multiple hits or convergent states for characters with high rates of homoplasy, as occurs with inadequate models for molecular data (Felsenstein 2004). Such effects undoubtedly occur with morphological data, particularly when matrices contain characters from different functional groups containing variable degrees of phylogenetic signal (Clarke and Middleton 2008; Lloyd et al. 2012), or characters with known histories of reversal (Pyron and Burbrink 2014). One promising approach is the automated detection of statistically identifiable partitions within morphological data sets that can be modeled with separate parameter estimates (Wright et al. 2015), similar to partitioning molecular data by gene and codon position. Another approach suggested by previous authors (Lewis 2001) and implemented in MrBayes (Nylander et al. 2004) involves a prior on the stationary frequency distribution of state labels (Wright et al. 2015).

Thus, a small shift in epistemological interpretation for appropriately coded characters meeting several criteria yields a significant advance in our approach to total-evidence phylogenetics. For characters that have been explicitly coded with respect to hypothesized or observed ancestral states or outgroup polarization (see reviews in Wiens 2000), we may treat the state labels as nonarbitrary observations of plesiomorphy and apomorphy, and thus estimate asymmetric transition rates. These asymmetric rates are well established for numerous characters, such as parity mode (Pyron and Burbrink 2014). Integrating these rates across characters should be relatively uncontroversial, as it models the biological reality of substitution dynamics for the observed character states using the MkA approach.

A very similar model was discussed by Klopstein et al. (2015), who used it to support directional evolution in morphological characters. These approaches are currently limited to binary characters. However, similar logic could be used to extend the MkA approach to multistate characters, particularly those that are ordered or have logically enforceable step matrices between states, presenting an avenue for future research. The only necessity (beyond computational implementation) is a logically

coherent framework for coding nonarbitrary state labels across characters, beyond presence/absence or plesiomorphy/apomorphy.

It is clear that morphological characters offer invaluable data sources for phylogenetic inference (Wiens 2004), though substantial challenges still remain for coding logically coherent character states (Pogue and Mickevich 1990) for extant and extinct taxa (Guillerme and Cooper 2016). Efforts to formalize morphological databases and character ontologies (Ramirez et al. 2007; Dececchi et al. 2015) should facilitate rapid development of suitable data sets. The relative impact of different priors (e.g., uniform, normal) for tip ages is unknown. The effects that fossil tips may have on estimates is unclear, and should be assessed in future studies. Encouragingly, recent authors have found that the large volume of missing cells typically observed for fossil taxa does not preclude relatively high accuracy and precision for their placement (Kearney and Clark 2003), particularly using Bayesian methods (Guillerme and Cooper 2015).

#### *The Phylogeny of Squamata*

A robust squamate phylogeny remains elusive, with disparate lines of evidence pointing in different directions (Conrad 2008; Wiens et al. 2010; Gauthier et al. 2012; Losos et al. 2012; Wiens et al. 2012; McMahan et al. 2015; Reeder et al. 2015). The volume of data also seems to have little impact, as the morphological and molecular results are similar across data sets of vastly different sizes both within and among partitions and studies (McMahan et al. 2015; Reeder et al. 2015). However, we can summarize present knowledge to highlight future research programs to directly address key nodes and the placement of crucial lineages.

In short, morphological data strongly support an earliest diverging Iguania, but offer poor resolution and obviously erroneous placement of many limbless taxa, particularly toward the species level (Conrad 2008; Gauthier et al. 2012). Molecular data strongly support a nested Iguania, but with occasional artifacts such as a paraphyletic Iguania, Scolecophidia, and Amphisbaenia (Castoe et al. 2009; Wiens et al. 2012), groups which are strongly supported by morphological data. For both data types, the apparent artifacts seem to stem from convergence. However, there are strong points of congruence between the data sets as well, in terms of the monophyly of most higher level extant taxa, and many aspects of their placement.

Broadly speaking, morphological and molecular data sets are roughly congruent with respect to the composition and relative relationships of Gekkota, Scincoidea, Lacertoidea (excluding Amphisbaenia), Anguimorpha, and Serpentes. The morphological tree can thus be transformed into the molecular tree by moving Iguania up three nodes (forming Toxicofera), moving Dibamidae down three nodes (with Gekkota), and moving Amphisbaenia down two nodes (with

Lacertoidea). The reverse is approximately true, as well. Confoundingly, there is morphological support for both an early-diverging and a nested Iguania (Reeder et al. 2015), as well as molecular support for an early-diverging or nested Iguania, or an early-diverging Lacertoidea (McMahan et al. 2015). In many combined data (Wiens et al. 2010; Reeder et al. 2015) and total-evidence analyses (Figs. 1–6), support for backbone nodes leading to a nested Iguania is low. Thus, choosing an “optimal” topology for Squamata becomes an exercise in weighing the relative strength of the different data sets and partitions (Losos et al. 2012).

Similar issues affect the fossil taxa coded in the matrices analyzed here. Variations or subsets of both of these matrices have been analyzed in uncalibrated, combined analyses by other researchers (Wiens et al. 2010; Reeder et al. 2015). However, several fossil taxa were treated by those authors as “rogues,” and one, *Sineoamphisbaena*, may be truly “rogue” (Aberer et al. 2013) in the sense of having a combination of irreconcilable character states and a large proportion of missing data, as noted by previous authors (Kearney 2003). Others such as *Huehuecuetzpalli* seem to have been apparent “rogues” since their topological placement was not enhanced by a timescale limiting the probable topologies.

Adding a timescale places *Huehuecuetzpalli* with Iguania using both matrices, albeit with weak support in most, but not all analyses (Figs. 1–6). This suggests that its numerous apparent plesiomorphies (Gauthier et al. 2012) are convergent. Placement with Iguania is also better supported by the age and geographic location of the fossil, which is corroborated by other recent discoveries of stem iguanians in the Neotropics (Simões et al. 2015). Wagner and Marcot (2013) discussed incorporating geographic sampling into divergence-time estimation; biogeographic models may be another area of future research for total-evidence dating.

For groups such as mosasaurs and polyglyphanodontids, simply adding temporal data does not resolve incongruence, with placements differing strongly between the CON and GEA matrices, analyzed both alone and with molecular data. Similar results are found for *Sineoamphisbaena* and *Eichstaettisaurus*. This highlights the problems of incongruence observed using different matrices, comprising different characters, scored by different researchers. Furthermore, it underscores the need described above for a unified set of character ontologies that standardize the observation of phylogenetically informative features across taxa and data sets. Even if we accept that the morphological data scored from fossil taxa are phylogenetically useful, it is crucial to document the nature of this signal, and quantify how placements vary with alternative character sampling and character-state coding.

The mechanisms of convergence that lead to discordance in squamates will be necessary to truly understand their evolutionary history. Either there has been a major episode of adaptive molecular



convergence resulting in erroneous genetic support for a nested Iguania, or there has been a massive episode of morphological convergence, resulting in erroneous phenotypic support for an early-diverging Iguania. One or the other seemingly must be true, but untangling the mechanisms and location of convergence will be necessary for resolution, and for interpreting the epistemological basis of phylogenetic signal contained in fragmentary fossil taxa in particular. A small-scale analysis of SINEs already provides some additional support for the molecular topology and a nested Iguania (Piskurek et al. 2006).

More morphological characters, including those drawn from previously understudied anatomical regions such as reproductive anatomy, may also be enlightening. For instance, cranial osteomorphology places Uropeltidae, Cyllindrophiiidae, and Anomochilidae (Old World) with Aniliidae (New World), and Tropidophiidae (New World) with advanced snakes (Hsiang et al. 2015). Contrastingly, molecular data strongly unite the New World tropidophiids and aniliids, placing the Old World taxa in an Old World clade with pythons (Wiens et al. 2008; Pyron and Burbrink 2012). Remarkably, this arrangement is supported by a soft-tissue synapomorphy, oviducts communicating with diverticuli of the cloaca rather than directly with the cloaca, uniting Tropidophiidae with Aniliidae and found in no other squamate (Siegel et al. 2011). Such disagreements are not uncommon among different anatomical regions (Clarke and Middleton 2008; Mounce et al. 2016), and isolating them may help uncover homoplasy and facilitate the removal of confounding phylogenetic artifacts (Davalos et al. 2014).

Congruence between molecular partitions and anatomical regions such as reproductive systems would be strong evidence for a robust resolution of squamate phylogeny, and homoplasy in the skeletal characters. However, skeletal data are not the only source of support for a basal Iguania (Reeder et al. 2015). It will be difficult to trust that combining morphological and molecular data negates homoplasy and accurately places fossils until the mechanisms driving the homoplasy are understood, and offending characters or partitions can be removed or handled appropriately (Davalos et al. 2014). The same is true for conflicting morphological character sets yielding alternate placements of fossil taxa, particularly in light of the strong epistemological and ontological problems with many of the characters used by both Conrad (2008) and Gauthier et al. (2012), which are described in detail by Simões et al. (2016, forthcoming). These are concerns that extend beyond squamates, and will likely affect most, if not all, attempts to build a unified Tree of Life.

#### SUPPLEMENTAL MATERIAL

Data available from the Dryad Digital Repository: <http://dx.doi.org/10.5061/dryad.dp3js>.

#### FUNDING

This research was funded by George Washington University and the Colonial One high-performance computing initiative, and US National Science Foundation [grants DBI-0905765 and DEB-1441719].

#### ACKNOWLEDGMENTS

For discussions of systematics, I thank J. Clark, J. Conrad, G. Hormiga, D. Lipscomb, D. Hillis, J. Gauthier, C. Hendry, N. Matzke, and F. Burbrink. For comments on this manuscript, I thank F. Anderson, T. Near, G. Slater, and A. Wright.

#### REFERENCES

- Aberer A.J., Krompass D., Stamatakis A. 2013. Pruning rogue taxa improves phylogenetic accuracy: an efficient algorithm and webservice. *Syst. Biol.* 62:162–166.
- Arcila D., Pyron R.A., Tyler J.C., Orti G., Betancur-R R. 2015. An evaluation of fossil tip-dating versus node-age calibrations in tetraodontiform fishes (teleostei: Percomorphaceae). *Mol. Phylogenet. Evol.* 82:131–145.
- Beck R.M.D., Lee M.S.Y. 2014. Ancient dates or accelerated rates? Morphological clocks and the antiquity of placental mammals. *Proc. R. Soc. B Biol. Sci.* 281:20141278.
- Benton M.J., Hitchin R., Wills M.A. 1999. Assessing congruence between cladistic and stratigraphic data. *Syst. Biol.* 48:581–596.
- Buckley T.R., Cunningham C.W. 2002. The effects of nucleotide substitution model assumptions on estimates of nonparametric bootstrap support. *Mol. Biol. Evol.* 19:394–405.
- Castoe T.A., de Koning A.P.J., Kim H.M., Gu W.J., Noonan B.P., Naylor G., Jiang Z.J., Parkinson C.L., Pollock D.D. 2009. Evidence for an ancient adaptive episode of convergent molecular evolution. *Proc. Natl. Acad. Sci. USA* 106:8986–8991.
- Clarke J.A., Middleton K.M. 2008. Mosaicism, modules, and the evolution of birds: results from a Bayesian approach to the study of morphological evolution using discrete character data. *Syst. Biol.* 57:185–201.
- Clyde W.C., Fisher D.C. 1997. Comparing the fit of stratigraphic and morphologic data in phylogenetic analysis. *Paleobiology* 23:1–19.
- Conrad J.L. 2008. Phylogeny and systematics of Squamata (Reptilia) based on morphology. *B. Am. Mus. Nat. Hist.* 310:1–182.
- Conrad J.L., Daza J.D. 2015. Naming and rediagnosing the Cretaceous gekkonomorph (Reptilia, Squamata) from Öösh (Övörkhangaï, Mongolia). *J. Vertebr. Paleontol.* 35:e980891.
- Conrad J.L., Norell M.A. 2006. High-resolution x-ray computed tomography of an early Cretaceous gekkonomorph (squamata) from Öösh (Övörkhangaï; Mongolia). *Hist. Biol.* 18:405–431.
- Davalos L.M., Velazco P.M., Warsi O.M., Smits P.D., Simmons N.B. 2014. Integrating incomplete fossils by isolating conflicting signal in saturated and non-independent morphological characters. *Syst. Biol.* 63:582–600.
- Dececchi T.A., Balhoff J.P., Lapp H., Mabee P.M. 2015. Toward synthesizing our knowledge of morphology: Using ontologies and machine reasoning to extract presence/absence evolutionary phenotypes across studies. *Syst. Biol.* 64:936–952.
- Donoghue M.J., Doyle J.A., Gauthier J., Kluge A.G., Rowe T. 1989. The importance of fossils in phylogeny reconstruction. *Ann. Rev. Ecol. Syst.* 20:431–460.
- Drummond A.J., Ho S.Y.W., Phillips M.J., Rambaut A. 2006. Relaxed phylogenetics and dating with confidence. *PLoS Biol.* 4:e699–710.
- Drummond A.J., Rambaut A. 2007. BEAST: Bayesian evolutionary analysis by sampling trees. *BMC Evol. Biol.* 7:214.
- Eernisse D.J., Kluge A.G. 1993. Taxonomic congruence versus total evidence, and amniote phylogeny inferred from fossils, molecules, and morphology. *Mol. Biol. Evol.* 10:1170–1195.

AQ7

- Estes R., de Queiroz K., Gauthier J. 1988. Phylogenetic relationships within Squamata. In: Estes R. and Pregill G., editors. *Phylogenetic relationships of the lizard families*. Stanford: Stanford University Press. p. 119–281.
- Farris J.S. 1982. Outgroups and parsimony. *Syst. Zool.* 31:328–334.
- Felsenstein J. 1992. Phylogenies from restriction sites: a maximum-likelihood approach. *Evolution* 46:159–173.
- Felsenstein J. 2004. *Inferring phylogenies*. Sunderland (MA): Sinauer Associates.
- Fisher D.C. 2008. Stratocladistics: integrating temporal data and character data in phylogenetic inference. *Ann. Rev. Ecol. Evol. Syst.* 39:365–385.
- Footo A.D., Liu Y., Thomas G.W.C., Vinar T., Alfoldi J., Deng J.X., Dugan S., van Elk C.E., Hunter M.E., Joshi V., Khan Z., Kovar C., Lee S.L., Lindblad-Toh K., Mancía A., Nielsen R., Qin X., Qu J.X., Raney B.J., Vijay N., Wolf J.B.W., Hahn M.W., Muzny D.M., Worley K.C., Gilbert M.T.P., Gibbs R.A. 2015. Convergent evolution of the genomes of marine mammals. *Nat. Genet.* 47:272–275.
- Fry B.G., Vidal N., Norman J.A., Vonk F.J., Scheib H., Ramjan S.F.R., Kuruppu S., Fung K., Hedges S.B., Richardson M.K., Hodgson W.C., Ignjatovic V., Summerhayes R., Kochva E. 2006. Early evolution of the venom system in lizards and snakes. *Nature* 439:584–588.
- Gauthier J., Kluge A.G., Rowe T. 1988. Amniote phylogeny and the importance of fossils. *Cladistics* 4:105–209.
- Gauthier J.A., Kearney M., Maisano J.A., Rieppel O., Behike A.D.B. 2012. Assembling the Squamate Tree of Life: perspectives from the phenotype and the fossil record. *B. Peabody Mus. Nat. Hist.* 53:3–308.
- Gavryushkina A., Welch D., Stadler T., Drummond A.J. 2014. Bayesian inference of sampled ancestor trees for epidemiology and fossil calibration. *PLoS Comp. Biol.* 10:e1003919.
- Giribet G. 2015. Morphology should not be forgotten in the era of genomics—a phylogenetic perspective. *Zool. Anz.* 256:96–103.
- Guillermé T., Cooper N. 2015. Effects of missing data on topological inference using a total evidence approach. *Mol. Phylogenet. Evol.* 94:146–158.
- Guillermé T., Cooper N. 2016. Assessment of available anatomical characters for linking living mammals to fossil taxa in phylogenetic analyses. *Biol. Lett.* 12:20151003.
- Harrison L.B., Larsson H.C.E. 2015. Among-character rate variation distributions in phylogenetic analysis of discrete morphological characters. *Syst. Biol.* 64:307–324.
- Heath T.A., Huelsenbeck J.P., Stadler T. 2014. The fossilized birth-death process for coherent calibration of divergence-time estimates. *Proc. Natl. Acad. Sci. USA* 111:E2957–E2966.
- Hennig W. 1966. *Phylogenetic systematics*. Urbana: University of Illinois Press.
- Hillis D.M., Moritz C., Mable B.K. 1996. *Molecular systematics*. 2nd ed. Sunderland (MA): Sinauer Associates.
- Holland S.M. 2016. The non-uniformity of fossil preservation. *Phil. Trans. R. Soc. B* 371:20150130.
- Hsiang A.Y., Field D.J., Webster T.H., Behlke A.D.B., Davis M.B., Racicot R.A., Gauthier J.A. 2015. The origin of snakes: revealing the ecology, behavior, and evolutionary history of early snakes using genomics, phenomics, and the fossil record. *BMC Evol. Biol.* 15:87.
- Huelsenbeck J.P. 1991. When are fossils better than extant taxa in phylogenetic analysis. *Syst. Zool.* 40:458–469.
- Huelsenbeck J.P. 1994. Comparing the stratigraphic record to estimates of phylogeny. *Paleobiology* 20:470–483.
- Huelsenbeck J.P., Rannala B. 1997. Maximum likelihood estimation of phylogeny using stratigraphic data. *Paleobiology* 23:174–180.
- Jones M.E.H., Anderson C.L., Hipsley C.A., Muller J., Evans S.E., Schöck R.R. 2013. Integration of molecules and new fossils supports a Triassic origin for Lepidosauria (lizards, snakes, and tuatara). *BMC Evol. Biol.* 13:208.
- Jukes T.H., Cantor C.R. 1969. *Evolution of Protein Molecules*. Academic Press: New York.
- Kass R.E., Raftery A.E. Bayes factors. *J. Am. Stat. Assoc.* 90:773–795.
- Kearney M. 2003. Systematics of the Amphisbaenia (Lepidosauria: Squamata) based on morphological evidence from recent and fossil forms. *Herpetol. Monogr.* 17:1–74.
- Kearney M., Clark J.M. 2003. Problems due to missing data in phylogenetic analyses including fossils: a critical review. *J. Vertebr. Paleontol.* 23:263–274.
- Kluge A.G. 1989. A concern for evidence and a phylogenetic hypothesis of relationships among *Epicrates* (Boidae, Serpentes). *Syst. Zool.* 38:7–25.
- Lanfear R., Calcott B., Ho S.Y.W., Guindon S. 2012. PartitionFinder: Combined selection of partitioning schemes and substitution models for phylogenetic analyses. *Mol. Biol. Evol.* 29:1695–1701.
- Lee M.S.Y. 2005a. Molecular evidence and marine snake origins. *Biol. Lett.* 1:227–230.
- Lee M.S.Y. 2005b. Squamate phylogeny, taxon sampling, and data congruence. *Org. Divers. Evol.* 5:25–45.
- Lee M.S.Y. 2009. Hidden support from unpromising data sets strongly unites snakes with anguimorph “lizards.” *J. Evol. Biol.* 22:1308–1316.
- Lee M.S.Y., Cau A., Naish D., Dyke G.J. 2014. Morphological clocks in paleontology, and a mid-Cretaceous origin of crown Aves. *Syst. Biol.* 63:442–449.
- Lee M.S.Y., Palci A. 2015. Morphological phylogenetics in the genomic age. *Curr. Biol.* 25:R922–R929.
- Lemmon A.R., Moriarty E.C. 2004. The importance of proper model assumption in Bayesian phylogenetics. *Syst. Biol.* 53:265–277.
- Lewis P.O. 2001. A likelihood approach to estimating phylogeny from discrete morphological character data. *Syst. Biol.* 50:913–925.
- Lipscomb D.L. 1992. Parsimony, homology and the analysis of multistate characters. *Cladistics* 8:45–65.
- Lloyd G.T., Wang S.C., Brusatte S.L. 2012. Identifying heterogeneity in rates of morphological evolution: Discrete character change in the evolution of lungfish (Sarcopterygii; Dipnoi). *Evolution* 66:330–348.
- Losos J.B., Hillis D.M., Greene H.W. 2012. Who speaks with a forked tongue? *Science* 338:1428–1429.
- McMahan C.D., Freeborn L.R., Wheeler W.C., Crother B.I. 2015. Forked tongues revisited: Molecular apomorphies support morphological hypotheses of squamate evolution. *Copeia* 103:525–529.
- Michevich M.F. 1982. Transformation series analysis. *Syst. Zool.* 31:461–478.
- Mounce R.C.P., Sansom R., Wills M.A. 2016. Sampling diverse characters improves phylogenies: craniodental and postcranial characters of vertebrates often imply different trees. *Evolution* 70:666–686.
- Mulcahy D.G., Noonan B.P., Moss T., Townsend T.M., Reeder T.W., Sites J.W., Wiens J.J. 2012. Estimating divergence dates and evaluating dating methods using phylogenomic and mitochondrial data in squamate reptiles. *Mol. Phylogenet. Evol.* 65:974–991.
- Nylander J.A.A., Ronquist F., Huelsenbeck J.P., Nieves-Aldrey J.L. 2004. Bayesian phylogenetic analysis of combined data. *Syst. Biol.* 53:47–67.
- O’Reilly J.E., dos Reis M., Donoghue P.C.J. 2015. Dating tips for divergence-time estimation. *Trends Genet.* 31:637–650.
- Orland K.E. 1997. Correlated rates of molecular and morphological evolution. *Evolution* 51:1381–1393.
- Parker J., Tsagkogeorga G., Cotton J.A., Liu Y., Provero P., Stupka E., Rossiter S.J. 2013. Genome-wide signatures of convergent evolution in echolocating mammals. *Nature* 502:228–231.
- Piskurek O., Austin C.C., Okada N. 2006. Sauria SINEs: Novel short interspersed retroposable elements that are widespread in reptile genomes. *J. Mol. Evol.* 62:630–644.
- Pogue M.G., Micevich M.F. 1990. Character definitions and character state delineation - the bete-noire of phylogenetic inference. *Cladistics* 6:319–361.
- Pyron R.A. 2011. Divergence time estimation using fossils as terminal taxa and the origins of Lissamphibia. *Syst. Biol.* 60:466–481.
- Pyron R.A. 2015. Post-molecular systematics and the future of phylogenetics. *Trends Ecol. Evol.* 30:384–389.
- Pyron R.A., Burbrink F.T. 2012. Extinction, ecological opportunity, and the origins of global snake diversity. *Evolution* 66:163–178.
- Pyron R.A., Burbrink F.T. 2014. Early origin of viviparity and multiple reversions to oviparity in squamate reptiles. *Ecol. Lett.* 17:13–21.
- Pyron R.A., Burbrink F.T., Wiens J.J. 2013. A phylogeny and revised classification of Squamata, including 4161 species of lizards and snakes. *BMC Evol. Biol.* 13:93.

- Ramirez M.J., Coddington J.A., Maddison W.P., Midford P.E., Prendini L., Miller J., Griswold C.E., Hormiga G., Sierwald P., Scharff N., Benjamin S.P., Wheeler W.C. 2007. Linking of digital images to phylogenetic data matrices using a morphological ontology. *Syst. Biol.* 56:283–294.
- Reeder T.W., Townsend T.M., Mulcahy D.G., Noonan B.P., Wood P.L., Sites J.W., Wiens J.J. 2015. Integrated analyses resolve conflicts over squamate reptile phylogeny and reveal unexpected placements for fossil taxa. *PLoS One* 10: e0118199.
- Rieppel O., Kearney M. 2002. Similarity. *Biol. J. Linn. Soc.* 75:59–82.
- Ronquist F., Huelsenbeck J.P. 2003. MrBayes 3: Bayesian phylogenetic inference under mixed models. *Bioinformatics* 19: 1572–1574.
- Ronquist F., Klopfstein S., Vilhelmsen L., Schulmeister S., Murray D.L., Rasnitsyn A.P. 2012. A total-evidence approach to dating with fossils, applied to the early radiation of the Hymenoptera. *Syst. Biol.* 61:973–999.
- Sereno P.C. 2007. Logical basis for morphological characters in phylogenetics. *Cladistics* 23:565–587.
- Siegel D.S., Miralles A., Aldridge R.D. 2011. Controversial snake relationships supported by reproductive anatomy. *J. Anat.* 218: 342–348.
- Simões T.R., Caldwell M.W., Kellner A.W.A. 2015. A new early Cretaceous lizard species from Brazil, and the phylogenetic position of the oldest known South American squamates. *J. Syst. Palaeontol.* 13:601–614.
- Simões T.R., Caldwell M.W., Palci A., Nydam R.L. 2016. Giant taxon-character matrices: quality of character constructions remains critical regardless of size. *Cladistics* (in press). doi: 10.1111/cla.12163.
- Slater G.J., Harmon L.J. 2013. Unifying fossils and phylogenies for comparative analyses of diversification and trait evolution. *Methods Ecol. Evol.* 4:699–702.
- Smith A. 1998. Is the fossil record adequate? Concluding remarks. *Nature Debates* 19th–24th December. Available from: [http://www.nature.com/nature/debates/fossil/fossil\\_frameset.html](http://www.nature.com/nature/debates/fossil/fossil_frameset.html)
- Stadler T. 2010. Sampling-through-time in birth-death trees. *J. Theor. Biol.* 267:396–404.
- Townsend T.M., Larson A., Louis E., Macey J.R. 2004. Molecular phylogenetics of Squamata: the position of snakes, amphisbaenians, and dibamids, and the root of the squamate tree. *Syst. Biol.* 53:735–757.
- Wagner P.J. 1995. Stratigraphic tests of cladistic hypotheses. *Paleobiology* 21:153–178.
- Wagner P.J. 1998. A likelihood approach for evaluating estimates of phylogenetic relationships among fossil taxa. *Paleobiology* 24: 430–449.
- Wagner P.J. 2000. The quality of the fossil record and the accuracy of phylogenetic inferences about sampling and diversity. *Syst. Biol.* 49:65–86.
- Wagner P.J., Marcot J.D. 2013. Modelling distributions of fossil sampling rates over time, space and taxa: assessment and implications for macroevolutionary studies. *Methods Ecol. Evol.* 4:703–713.
- Wiens J.J. 1998. Combining data sets with different phylogenetic histories. *Syst. Biol.* 47:568–581.
- Wiens J.J. 2000. *Phylogenetic analysis of morphological data*. Washington, DC: Smithsonian Institution Press.
- Wiens J.J. 2004. The role of morphological data in phylogeny reconstruction. *Syst. Biol.* 53:653–661.
- Wiens J.J., Bonett R.M., Chippindale P.T. 2005. Ontogeny discombobulates phylogeny: paedomorphosis and higher-level salamander relationships. *Syst. Biol.* 54:91–110.
- Wiens J.J., Chippindale P.T., Hillis D.M. 2003. When are phylogenetic analyses misled by convergence? A case study in Texas cave salamanders. *Syst. Biol.* 52:501–514.
- Wiens J.J., Hutter C.R., Mulcahy D.G., Noonan B.P., Townsend T.M., Sites J.W., Reeder T.W. 2012. Resolving the phylogeny of lizards and snakes (Squamata) with extensive sampling of genes and species. *Biol. Lett.* 8:1043–1046.
- Wiens J.J., Kuczynski C.A., Smith S.A., Mulcahy D.G., Sites J.W., Townsend T.M., Reeder T.W. 2008. Branch lengths, support, and congruence: testing the phylogenomic approach with 20 nuclear loci in snakes. *Syst. Biol.* 57:420–431.
- Wiens J.J., Kuczynski C.A., Townsend T., Reeder T.W., Mulcahy D.G., Sites J.W. 2010. Combining phylogenomics and fossils in higher-level squamate reptile phylogeny: molecular data change the placement of fossil taxa. *Syst. Biol.* 59:674–688.
- Wilcox T.P., de Leon F.J.G., Hendrickson D.A., Hillis D.M. 2004. Convergence among cave catfishes: long-branch attraction and a bayesian relative rates test. *Mol. Phylogenet. Evol.* 31:1101–1113.
- Wood H.M., Matzke N.J., Gillespie R.G., Griswold C.E. 2013. Treating fossils as terminal taxa in divergence time estimation reveals ancient vicariance patterns in the palpimanoid spiders. *Syst. Biol.* 62: 264–284.
- Wright A.M. 2015. Estimating phylogenetic trees from discrete morphological data [PhD Thesis]. [EEB]: The University of Texas Austin, TX.
- Wright A.M., Lyons K.M., Brandley M.C., Hillis D.M. 2015. Which came first: the lizard or the egg? Robustness in phylogenetic reconstruction of ancestral states. *J. Exp. Zool. Part. B* 324:504–516.
- Wright A.M., Hillis D.M. 2014. Bayesian analysis using a simple likelihood model outperforms parsimony for estimation of phylogeny from discrete morphological data. *PLoS One* 9: e109210.
- Wright A.M., Lloyd G.T., Hillis D.M. 2015. Modeling character change heterogeneity in phylogenetic analyses of morphology through the use of priors. *Syst. Biol.* doi: 10.1093/sysbio/syv122.
- Xie W., Lewis P.O., Fan Y., Kuo L., Chen M.-H. 2011. Improving marginal likelihood estimation for Bayesian phylogenetic model selection. *Syst. Biol.* 61:150–160.
- Zhang C., Stadler T., Klopfstein S., Heath T.A., Ronquist F. 2015. Total-evidence dating under the fossilized birth-death process. *Syst. Biol.* 65:228–249.

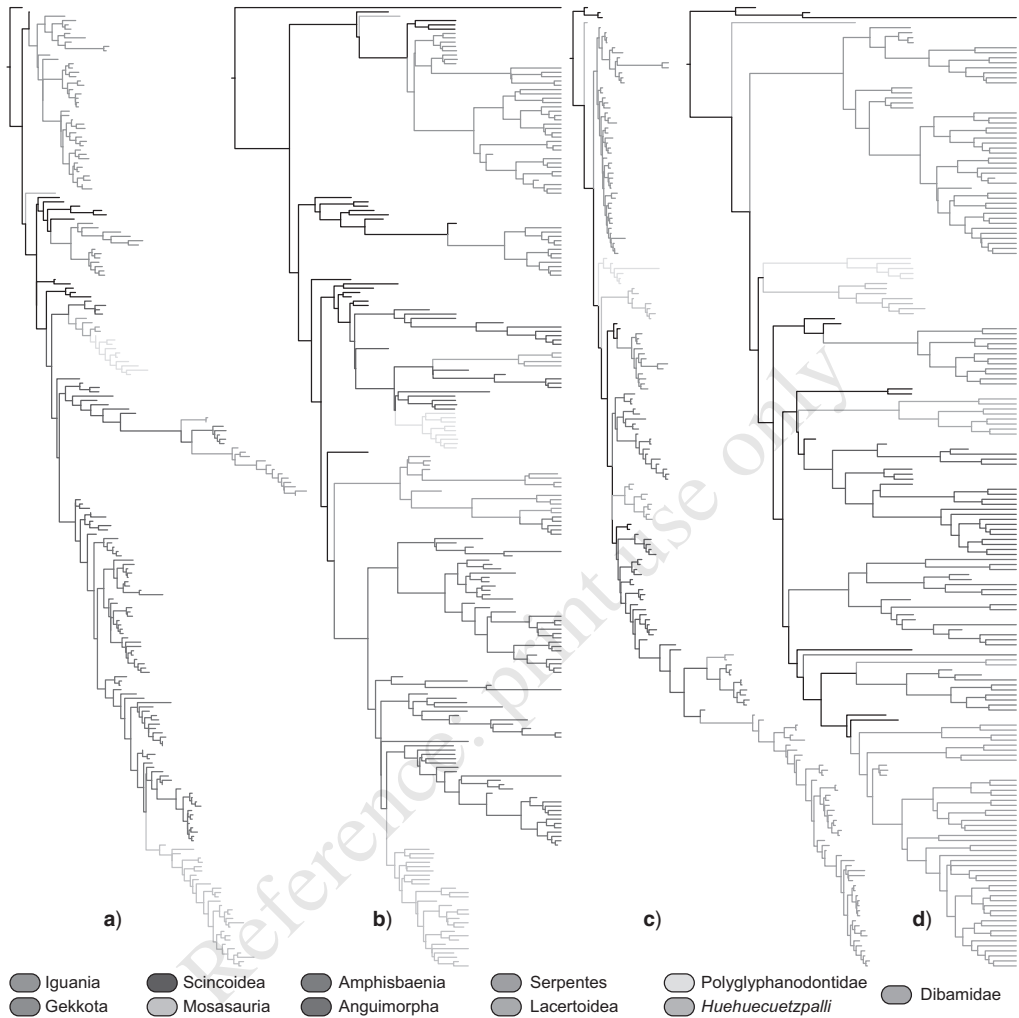


FIGURE 1.

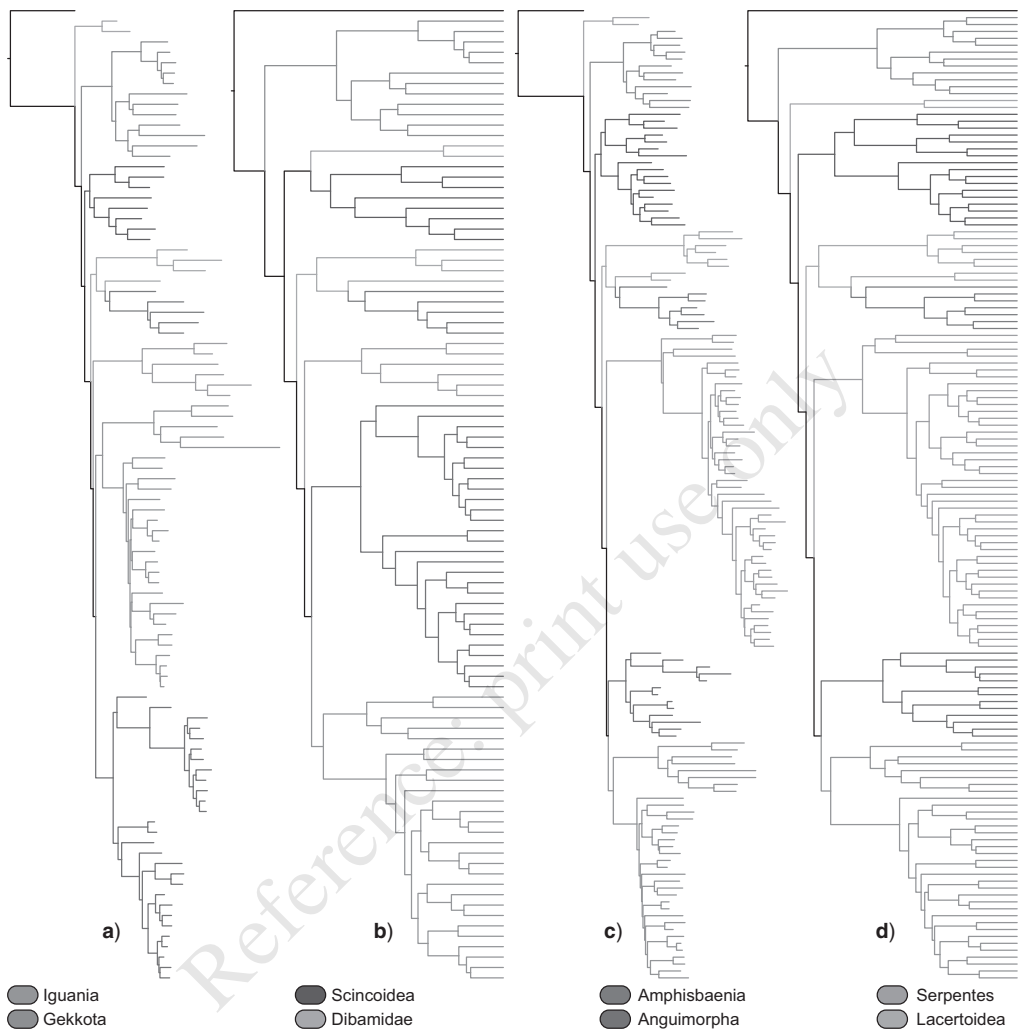


FIGURE 2.



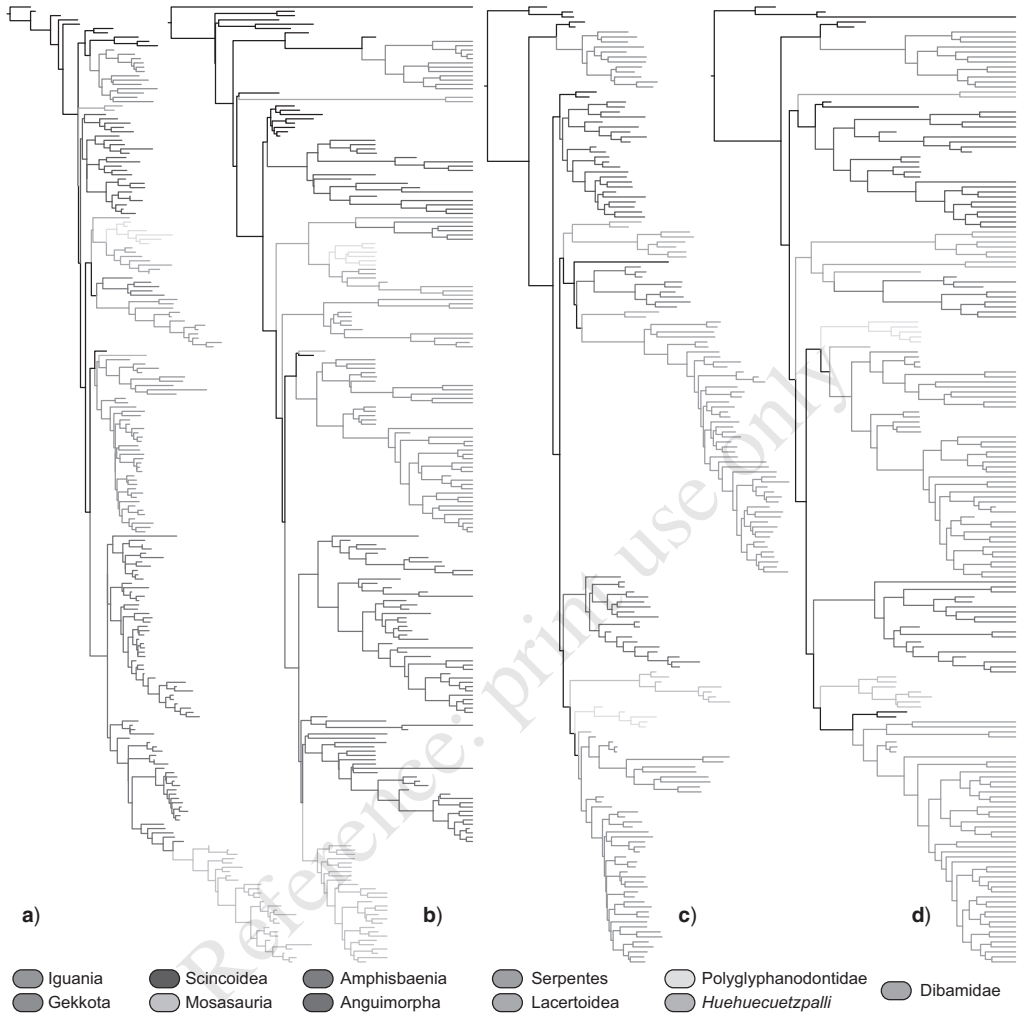


FIGURE 3.



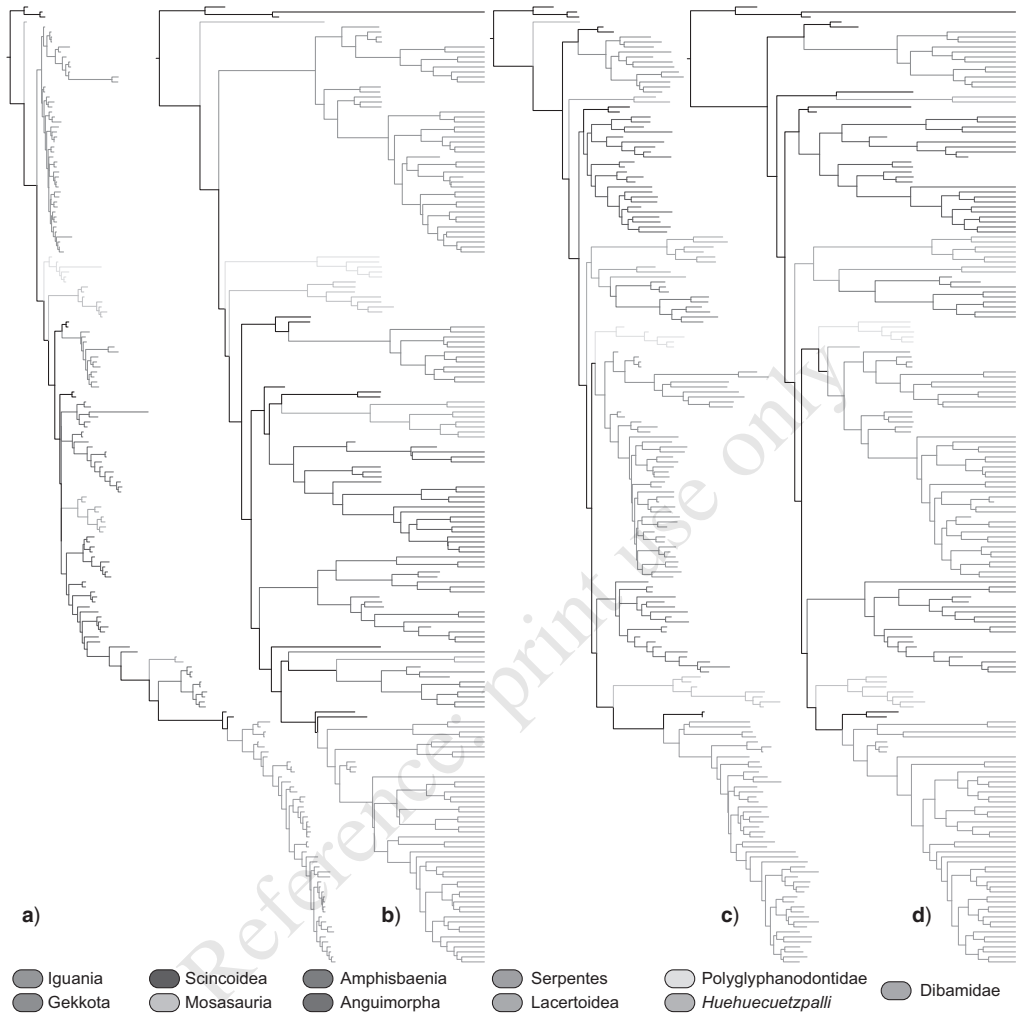


FIGURE 5.

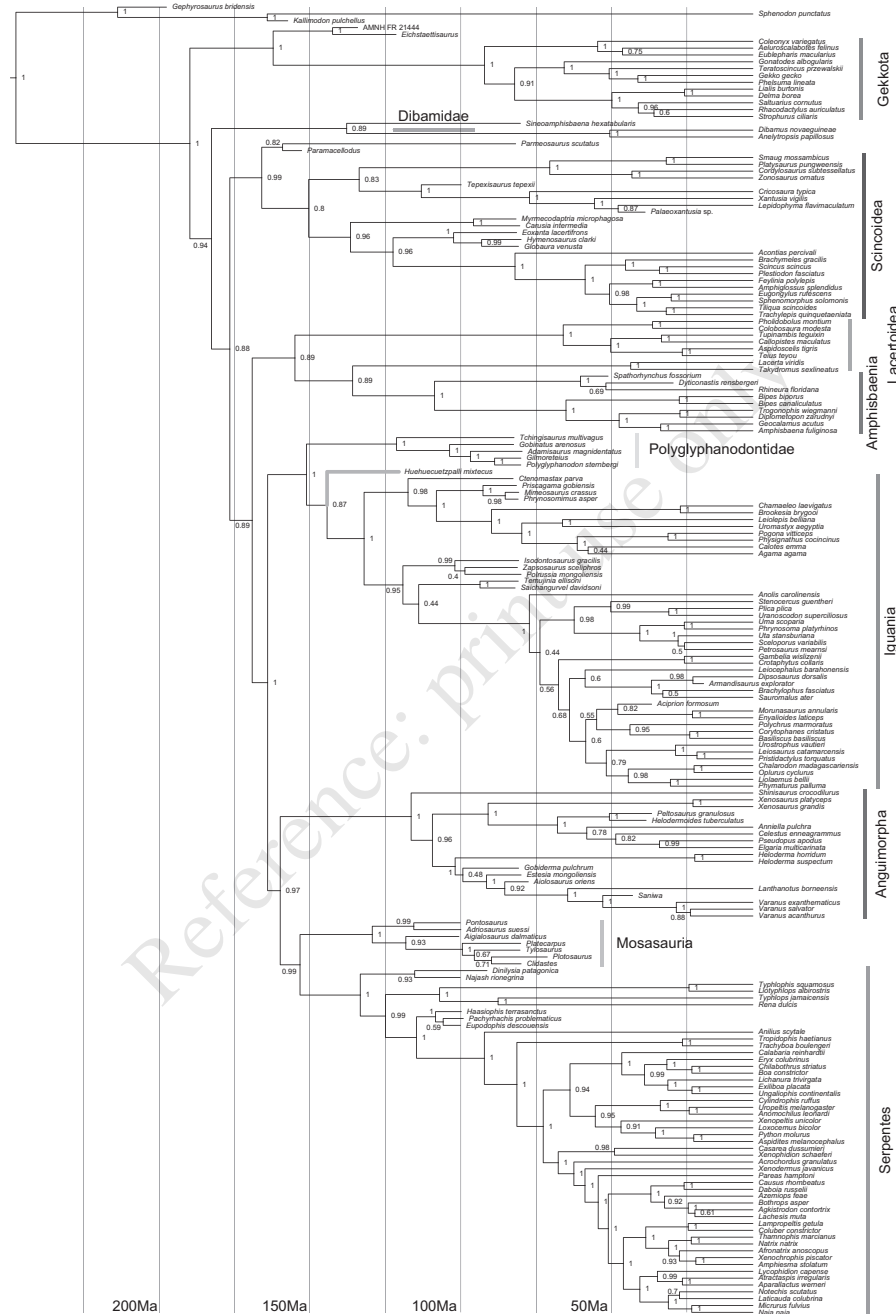


FIGURE 6.